Title
A Tasteful Study of the Drosophila Mushroom Body

Author
Chia, Justine

Publication Date
2019

Peer reviewed|Thesis/dissertation

A Tasteful Study of the *Drosophila* Mushroom Body

By Justine X Chia

A dissertation submitted in partial satisfaction of the

requirements for the degree of

Doctor of Philosophy

In

Molecular and Cell Biology

in the

Graduate Division

of the

University of California, Berkeley

Committee in charge:

Professor Kristin Scott, Chair
Professor Marla Feller
Professor Diana Bautista
Professor Silvia Bunge

Summer, 2019

Abstract

A Tasteful Study of the *Drosophila* Mushroom Body

by

Justine X Chia

Doctor of Philosophy in Molecular and Cell Biology

University of California, Berkeley

Professor Kristin Scott, Chair

Learning to distinguish 'good' from 'bad' is essential to an animal's survival. Taste compounds have intrinsic value to animal survival and serve as innate rewards and punishments. From humans to flies, nutritious substances like sugar are intrinsically positive and promote acceptance behavior, whereas potentially toxic bitter substances like quinine, for example, are met with disgust and aversion. Yet, even the strongest instinctual behavioral drives such as feeding can be modified by prior associations. How does this learning happen? Using the model organism *Drosophila Melanogaster*, I investigated how the inputs and outputs of a learning center can modulate feeding behavior.

In the first part of this dissertation, I investigated the modulation of proboscis extension by inputs and outputs of the learning center (mushroom body, MB) in the fly brain. I identified 10 split-Gal4 lines that cover 7 different cell types of MB output neurons (MBONs) that decrease the probability of proboscis extension when activated. Silencing these neurons had modest effects on proboscis extension. Additionally, I found 3 split-Gal4 lines labeling dopaminergic neurons (DANs) that decrease proboscis extension to sucrose, upon activation. I also found that the MBONs which suppress proboscis extension upon activation do not respond to sucrose. Lastly, I describe areas for putative neurons that are downstream of MBONs.

In the second part of this dissertation, I outline the methods I developed for a large-scale calcium imaging experiment to track neuronal changes during an aversive taste conditioning paradigm. While this set of experiments was ultimately inconclusive because we lacked a good positive control and behavioral readout to determine successful learning in our *in vivo* prep, we believe that outlining the experimental methods and analysis pipeline may be useful and applicable for more general analysis of large-scale calcium imaging endeavors to answer questions about neuronal changes during a behavior.

Overall, my thesis research investigated how the activity of MB inputs and outputs impinges on feeding behavior by characterizing mushroom body neurons that antagonize feeding behavior and examining how they alter activity in feeding circuits. The work described in this thesis provides insight into how the mushroom body flexibly alters the response to taste compounds and modifies feeding decisions.

To my friends and family.

TABLE OF CONTENTS

Acknowledgements

First and foremost I would like to thank my advisor Kristin Scott, for her unwavering support and mentorship over the past 6 years. My PhD journey would not have been possible without her advice and encouragement. Her door is (literally) always open, and I have learned so much about scientific writing, critical thinking, and experimental design. I am especially grateful for her being open to new experiments and ideas, as well as being supportive of exploration of creative strategies to overcome scientific setbacks. I am also grateful for her guidance during periods of seemingly too much lateral motion, and for her feedback throughout the writing of my dissertation.

One piece of advice that I received while trying to choose a lab for my thesis work was to choose somewhere that I would be excited about getting up and going to work every morning. I really won the lottery with the Scott lab. I couldn't have asked for a more collaborative, supportive, and fun environment. I could always rely on my labmates for advice and fly room banter. I am eternally grateful everyone for fruitful scientific discussions, as well as general wisdom and support. All members of the Scott lab, past and present, have in some way contributed to my thesis work: Carolina Reisenman, Salil Bidaye, Amanda Gonzalez, Phil Shiu, Ellie Sterne, Zepeng Yao, Sarah Leinwand, Maggie Laturney, Stef Engert, Molly Kirk, Hyesoo Youn, Nick Jourjine, Samantha Cheung, Heesoo Kim, Dave Harris, Brendan Mullaney, Christoph Scheper, Ben Kallman, Colleen Kirkhart, and Rob Thistle.

I am also grateful for my classmates and the neuroscience community at Berkeley. In particular, my 'neurotons' Katie Benthall, Carolyn Walsh, and Corey Webster have been great friends throughout all the milestones and hurdles of grad school. Also from my neuro cohort, Dylan Paiton helped me with data analysis for some experiments in Chapter 2. The helpful administrative staff, in particular Berta Perra, helped me navigate course enrollment and drop deadlines. I would also like to thank my thesis committee (Marla Feller, Diana Bautista, and Silvia Bunge) for their insights and feedback on my science, and advice for future scientific endeavors.

I would also like to acknowledge my friends outside of my immediate academic community. Stephanie Wuerth and Clara Eng, thank you for inspiring me to keep running. Hetul Patel, thank you for making me a 13A belayer. Paul Laskowski, thank you for all of your feedback and help with statistics and R problems, for all your support through all the late nights and weekends in lab, and for being my biggest cheerleader. Thank you to my adventure crew (April, Milli, Christina, Ellen, and Jess) for being there for me and cheering me on. I would also like to give a quick nod to the design community at UC Berkeley, in particular Chris Meyers and Kuan-ju Wu at the Citris Invention lab - I've learned so much about design and fabrication and making.

Last, but certainly not least, I would like to thank my family their love and support. Throughout my entire life, my parents Stanley and Faith Chia have encouraged me to be creative and diligent in my studies, and have inspired me to be the best possible version of myself. I am incredibly grateful for the opportunities that they gave me.

Chapter 1

Introduction

The smell of barbeque chicken pizza wafting through the air could be mouthwateringly tantalizing for the hungry graduate student in search of free food, or it could be repulsive, reminiscent of a week-long food poisoning stint many months ago. The way in which we respond to an external stimulus is determined by a complex interplay between innate drives and prior experience. At their most basic level, our memories are what make us who we are, direct our behavior, and allow us to plan for the future based on past experience. We exist in a present that is in a constant flux of becoming our past and as the future lies before us, we move forward with our remembered experience to help guide us. But what *are* memories? How do nervous systems allow for such flexible processing of sensory information? Can I learn to like cilantro? How does a change in synaptic strength result in such powerful associations between smells, tastes, and life events from years ago? How does information flow from sensory input to motor output, and how is that modified? To even begin to understand learning and memory in animals, we must first understand the conditions that lead to a learned behavior. We need to understand the molecular mechanisms that facilitate memory encoding and storage. We need to understand the neural circuitry that underlies sensory processing and plasticity, and the circuit that ultimately drives motor output. To investigate these inherently complicated processes, scientists rely on model organisms. Studies in rodents and primates provide insights into sensory processing and learned associations, but the complex brain organization makes it difficult to understand the entire flow of information from sensory input to learning centers to motor output. As such, many researchers turn to organisms with simpler nervous systems, such as the sea snail *Aplysia*, or the fruit fly *Drosophila Melanogaster*, with the hope that discoveries made in these organisms will provide insights into principles conserved across species.

The example of feeding behavior shows that even instinctual drives that are essential for survival can be modified by prior associations. Taste compounds have intrinsic value to animal survival and serve as innate rewards and punishments. From humans to flies, nutritious substances like sugar promote acceptance behavior, whereas potentially toxic bitter substances like quinine, for example, are met with disgust and aversion. Yet, a single pairing of a sweet substance with an aversive stimulus is capable of producing strong avoidance of this innately rewarding stimulus (1). In fact, conditioned taste aversion is unique among associative learning paradigms for the unusual robustness of the memory it produces (2, 3).

Memory in *Drosophila*

Progress in understanding the neural mechanisms of learning and memory has come from studies in several organisms. Some animal models were initially chosen because of a unique experimental strength, such as large accessible cells that facilitate cellular and physiological analyses, or complex circuits that more closely resemble those present in humans. The fly brain is uniquely positioned as a model organism to probe the neural mechanisms underlying learning and behavior. There is an abundance of genetic tools available for labeling and manipulating neural circuits that makes *Drosophila* an attractive system. These tools allow for precise manipulation of single neurons to study behavioral changes, as well as allow for physiological recordings from identified

neurons, with both electrophysiology and functional imaging. Moreover, with only 100,000 neurons, (as compared to ~10^8 in a mouse or ~10^11 in a human) the nervous systems of flies are much more tractable than mammalian brains. Fly brains are simpler, yet they are still capable of producing complex behaviors, as well as a wide array of learned associations such as classical and operant conditioning, habituation, dishabituation, and sensitization (4).

Flies use diverse sensory inputs for learned associations. Perhaps one of the more ethological forms of associative memory studied in flies is courtship conditioning. In courtship conditioning, a naive male fly learns to suppress his innate instinct to court after being continuously rejected by a mated female. The male maintains this memory even when placed in the presence of a virgin female, which is receptive to mating. Courtship behavior is complex and engages multiple sensory systems, so the exact nature of the associative cue is unknown, although contact with female pheromones is thought to be important (5). Flies can also learn to recognize and respond to visual patterns, colors, and intensities (6). They can also form associative memories with auditory cues (7) or tastes (8–11).

Over the last half-century, the form of learning that has been most widely studied in *Drosophila* is olfactory associative memory (12, 13). In olfactory associative learning, flies associate odors with an aversive cue such as shock, heat, or bitter taste, or a rewarding cue such as sugars or water (14–17). After training, they either approach an odor if it was paired with a reward or avoid an odor if paired with an electric shock as punishment. Learning is most often measured by providing flies with a choice between a trained odor and untrained odor in a T-maze, and recording the population preference.

The site for associative learning in *Drosophila*, as well as many other insects, has long been thought to be a higher brain region called the mushroom body (MB). The MB is a bilateral structure (i.e. there is one mushroom body per hemisphere) but the pair as a whole is often referred to as the MB. Ablation and neural silencing experiments have shown that the MB is essential for the formation, consolidation, and retrieval of olfactory memory (18, 19). For example, flies with genetic mutations that alter the structure of the MB, as well as flies with chemically ablated mushroom bodies, fail to learn (18).

How does sensory information reach the MBs in the higher brain? In the olfactory circuit of the fly, the neurons upstream of the MB have been well studied. Flies have 2 organs that detect volatile chemicals: the antennae and the maxillary palps. Olfactory receptor neurons (ORNs) carry information from these organs to the antennal lobes, where their projections are organized into about 50 glomeruli; each glomerulus contains dendrites of projection neurons (PNs) that then carry information to the higher brain (20, 21). PNs project to two anatomical regions, the lateral horn (LH) and the calyx of the mushroom body (MB). The axons of olfactory PNs are divided into multiple tracts. The majority of excitatory PNs follow the inner antenno-cerebral tract (iACT), synapsing first in the MB, then projecting into the LH. In contrast, the inhibitory PNs of the medial ACT (mACT) project solely to the LH, and the small number of neurons that form the outer ACT (oACT) project first to the LH, then to the calyx of the MB (21–24). The MB is where the sensory information from PNs converges with reward or punishment signals conveyed by dopaminergic inputs; the integrated signal is relayed by MB output neurons to many brain regions to ultimately drive motor behaviors.

Mushroom body organization

The mushroom body is beautifully organized. The intrinsic cells of the MB are called Kenyon cells, and there are about 2000 of them in each hemisphere (25, 26). Kenyon cells are subdivided into three major subtypes (α/β, α'/β' and γ) based on anatomy, developmental order (27), and levels of gene expression (28). The axons of KCs bundle to form the horizontal and vertical lobes of the MB. Unlike the α/β and α'/β' neurons, which bifurcate and send processes into both the horizontal and vertical lobes, the γ neurons project exclusively to horizontal lobes. [Fig. 1.1] These lobes are the output site of the MB, where information is read and relayed by the MB by mushroom body output neurons (MBONs). Our understanding of the MB was advanced in 2014, when a highly specific set of genetic tools for neurons of the MB was published. In this study, the majority of neurons associated with the MB were identified and thoroughly characterized, confirming previous studies that proposed a modular and highly organized architecture (26). These tools allowed for manipulation of specific neurons in the MB, paving the path for more precise dissection of the circuitry of this learning and memory center.

Surprisingly, the thousands of intrinsic and extrinsic neurons of the MB converge onto fewer than 40 MBONs per hemisphere, characterized into 21 distinct cell types based on morphology [Fig 1.1]. Anatomical analysis shows that the dendrites of each type of MBON innervate only a small section of the MB lobes, creating a tiled pattern of compartments with very little overlap. This tiling pattern mirrors the tiling pattern of dopaminergic inputs that relay reward or punishment signals to the MB lobes [Fig 1.1]. This neat compartmental organization could potentially explain how a relatively small number of reinforcement and output neurons are able to code for such a large repertoire of specific associations.

The good, the bad, and the dopamine

The central neuromodulator for learning in flies is thought to be dopamine, and dopaminergic neurons (DANs) deliver the valence (positive or negative) of a stimulus to the MB.

Most of the DANs in the MB have bilaterally symmetric axonal innervations to the MB lobes (26). Interestingly, direct activation of DANs can substitute for the unconditioned stimulus (US) to induce learning (9, 10, 29–32).

Distinct types of DANs mediate either aversive or appetitive learning (32). The two subpopulations involved in associative odor learning are the posterior paired lateral 1 (PPL1) cluster and the protocerebral anterior medial (PAM) cluster. The PPL1 cluster consists of 12 neurons that tile the MB lobes with non-overlapping projections, a pattern which overlaps with the projections of some of the MBONs (26). If these neurons are silenced, flies are not capable of forming aversive memories and activating these neurons during odor presentation is sufficient for memory formation (30). These data strongly suggest that PPL1 neurons are responsible for delivering the US signal for aversive odor learning. PAM neurons, on the other hand, have been implicated as the positive US in appetitive learning, as silencing them disrupts appetitive learning and activating them

induces appetitive learning. Calcium imaging studies have also demonstrated that these neurons are activated by sugar ingestion (32).

Valence coding by MBONs

MBONs are thought to signal the predictive value of a given stimulus. According to this model, when a fly encounters certain overlapping stimuli in the environment, such as a neutral odor and a noxious shock, conditioned stimulus (CS) and US signals will be relayed to the MB by projection neurons and DANs, respectively. The coincident detection of these signals in the MB lobes will then modify the synaptic strength between KCs and MBONs, change the response profile of the MBON, and bias behavioral selection. In the case of olfactory aversive learning, learning increases the likelihood of future avoidance.

The behavioral roles of MBONs have been investigated through direct activation (33, 34). Flies expressing a red-light-gated channel in the different subsets of MBONs were given a choice between dark and red light. Activation of some MBONs caused flies to prefer red light, whereas activation of other MBONs caused flies to avoid red light. Thus, individual MBONs can drive innate approach or avoidance behavior by signaling a positive or negative valence (33). In addition, activation of some MBON subsets had no discernible effect in this assay.

The finding that MBONs drive acceptance or avoidance is one piece of evidence that underlies the current model of the MB function. This model proposes that there are appetitive memory compartments and aversive memory compartments and the balance of activity in the appetitive and aversive compartments determines behavior. Studies of the function and activity of DAN inputs and MBON outputs that arborize in the same MB compartment are revealing nuances of how activity changes upon learning. These studies show that a DAN input signaling sugar reward synapses on the same compartment as an MBON that drives aversion (33). Pairing an odor with a sugar reward leads to inhibition of the aversive MBON, leading to increased attraction. Similarly, punishment DAN inputs synapse on the same compartments as MBONs that drive attraction. The model that emerges is that DAN inputs inhibit MBON outputs through long-term depression (LTD) to bias behavior.

Evidence for LTD at the MBON comes from studying memory traces in these compartments with electrophysiology as well as functional imaging, in conjunction with artificial activation of DANs using specific genetic drivers. *In vivo* whole-cell recordings in MBONs show that responses to odors were greatly decreased after odor-dopamine pairing (35). This plasticity is sensitive to the order of activation (odor presentation followed by DAN activation induces robust attenuation of activity, while the reverse resulted in no changes.) Additionally, the effect is also spatially specific – recordings from neighboring compartments showed no plasticity (35). Because the activity in MBONs decreased, it was concluded that KC-MBON synapses undergo LTD.

To summarize our current understanding, sensory (olfactory) information is processed by multiple, independent compartments of the mushroom body. During learning, each compartment receives olfactory information from KCs as well as reward and punishment signals through DANs, and each compartment outputs to specific

MBONs. Each one of these compartments functions to assign valence to an odor. In a naïve or 'neutral' animal, the total valence balances out with all the positive and negative compartments, and thus there is no approach or avoidance behavior observed. During aversive learning, the balance is tipped toward the negative side to trigger avoidance behavior: LTD decreases the output in a compartment that signals positive valence. This happens with multiple compartments – experimental evidence shows that activating multiple MBONs results in a more robust behavior phenotype (33). Why are there so many compartments? It is possible that the different compartments are responsible for different aspects of memory, for example the robustness of the memory, or the type of sensory memory.

Taste conditioning

Although we have yet to fully identify the input pathway to the MB (some second order neurons have been identified as pathways to the higher brain, as discussed above), it is clear that taste information reaches the MB and is encoded in a way that allows for it to play multiple roles in memory formation. In addition to serving as US in olfactory learning paradigms, tastants can also be used as the CS in taste conditioning experiments, and learning may follow a similar logic as olfactory conditioning. Like odors, taste activates a small number of KC dendrites in the MB calyx (9), as shown through calcium imaging experiments.

In taste conditioning, flies can be trained to reject sweet tastants. The CS could be a noxious stimulus such as pulse of heat from an infrared laser (8), a bitter substance (9, 11), or even artificial activation of bitter-sensing neurons (36).Thus, tastants can serve as a CS, US, or both in associative memory paradigms.

Taste learning is an excellent domain for the study of learning and memory, since the sensory input into the central brain as well as region for motor output are well-defined. However, the pathways for taste information to reach the MBs are have not been fully described, and neither have the pathways that convey information back down from the higher brain to drive the feeding motor behavior. An understanding of the pathway downstream of the MB would provide insights into how learning centers modify motor programs.

How does a fly taste?

Fruit flies detect tastes with sensory neurons on the proboscis, internal mouthparts, legs, wings, and ovipositor (21). Feeding behavior usually begins when the legs come into contact with food. When a fly encounters an appetitive substance such as sugar with its legs, it stops and extends its proboscis, spreads its labellum and begins ingesting. Ingestion is prolonged by activation of internal mouthpart neurons. This feeding motor program involves the cooperation of multiple gustatory neurons (37).

The sensory structures that detect taste compounds are chemosensory bristles that contain two to four gustatory receptor neurons (GRNs) that respond to nonvolatile chemicals in the environment, as well as a mechanosensory neuron. The GRNs are

located at the base of the gustatory bristle and send a dendrite into the shaft of the bristle where it comes into contact with chemicals in food sources (38). Electrophysiological recordings of gustatory bristles indicate that different classes of neurons in a bristle respond selectively to bitter compounds, sugars, salt, or water (39–41).

Taste compounds are detected via distinct gustatory receptor (GR) proteins expressed in GRNs (42, 43). The GR family contains 68 members, most of which are expressed in the taste sensilla (44, 45). The GRs are grouped according to their co-expression patterns and responses to taste compounds. For example, gustatory receptors Gr5a and Gr64f detect sweet tastes and are expressed exclusively in sweet-sensitive GRNs (46, 47), whereas the bitter GRs such as Gr66a are expressed exclusively in bitter-sensitive GRNs. In addition to detecting bitter taste, Gr66a-expressing neurons can also detect high salt taste, which is also aversive to flies (48).

The *Drosophila* gustatory system also has detection mechanisms for carbonation and salt taste, through members of the ionotropic receptor (IR) family of ion channels (49, 50). The 66 IRs that have been identified in *Drosophila* serve diverse functions in the olfactory system, and their expression in GRNs has not been exhaustively characterized. About 33 members of the IR family (the Ir20a clade) have been found in GRNs, with at least one member of the family expressed in almost all taste sensilla (51). Another IR expressed in taste tissue, Ir76b, has been implicated in the detection of salt taste and amino acid taste (50, 52, 53).

Contact chemosensation is also mediated by another class of taste receptors encoded by a few members of the Pickpocket (PPK) family of ion channels. PPK is the *Drosophila* equivalent of the Deg/ENaC superfamily , which have been found in nematodes, flies, snails, and vertebrates, and have been implicated a broad spectrum of cellular functions including mechanosensation, proprioception, pain sensation, gametogenesis, and epithelial Na+ transport (54, 55). PPK28 acts as an osmosensitive ion channel that detects water (56, 57); PPK23, PPK25 and PPK29 mediate contact pheromone detection (58–61).

The majority of sensory neurons on the legs and wings project to the ventral nerve cord (VNC), whereas those on the proboscis and mouthparts send axons to the subesophageal zone (SEZ) of the central brain, the primary region for gustatory information processing (21, 47, 62, 63). Several second-order taste neurons and their functions have been identified and characterized: One bilateral pair of candidate gustatory second-order neurons (G2Ns) are local SEZ interneurons (64). Another set of second-order sugar GRNs project to a brain region called the antennal mechanosensory and motor center (AMMC) (65). An additional set of candidate second-order gustatory neurons includes 12 cholinergic local interneurons (IN1) that respond during sucrose ingestion, and promote ingestion with exogenous activation (37). Most recently, 3 different classes of second-order taste neurons called taste projection neurons (TPN) have been identified (63). Two classes of TPNs project to the superior lateral protocerebrum (SLP) and convey bitter taste information to MB learning circuits; interestingly, these neurons are required for conditioned taste aversion (63). Together, these studies suggest modality-specific pathways, consistent with a labeled line view of taste processing.

Overall, the organization of taste detection in *Drosophila* is similar to that of the mammalian taste system (66). In both cases, there are only a few categories of taste cells, and activation of these cells drives innate acceptance or rejection behavior. This

organization allows for the detection of many compounds (via many receptors) to drive a select few innate behaviors.

Results and Contributions

While some of the circuitry for innate taste detection and feeding behavior has been established, the mechanism through which learning centers modify this pathway is not known. The main goal of this dissertation is to shed light on this aspect of learning through a series of *Drosophila* experiments.

In the first part of this dissertation, I investigate the modulation of proboscis extension by inputs and outputs of the MB in the fly brain. I identify 10 MBON-split-Gal4 lines covering 7 different cell types that decrease the probability of proboscis extension to sucrose when they are optogenetically activated. Additionally, I find 3 DANs that decreased proboscis extension upon activation. One compartment overlaps between the MBONs and DANs that influence proboscis extension. Using calcium imaging, I find that the MBONs that suppress proboscis extension upon activation do not respond to sucrose. Lastly, I use the genetically encoded anterograde synaptic tracing tool *trans*-Tango to find areas for putative neurons that are downstream of MBONs.

In the second part of this dissertation, I outline a set of methods for a large-scale calcium imaging experiment to track neuronal changes during an aversive taste conditioning paradigm. While the lack of a good positive control and inconsistent behavioral readout means that it is not possible to draw definitive conclusions about neuronal changes that occur during learning, I believe that outlining the experimental methods and analysis pipeline may be useful and applicable for more general analysis of large-scale calcium imaging data.

Overall, my thesis research investigates how the activity of MB inputs and outputs impinges on feeding behavior by characterizing mushroom body neurons that antagonize feeding behavior and examining how they alter activity in feeding circuits. Through these methods, I provide new insight into how the mushroom body flexibly alters the response to taste compounds and modifies feeding decisions.

Figure 1.1

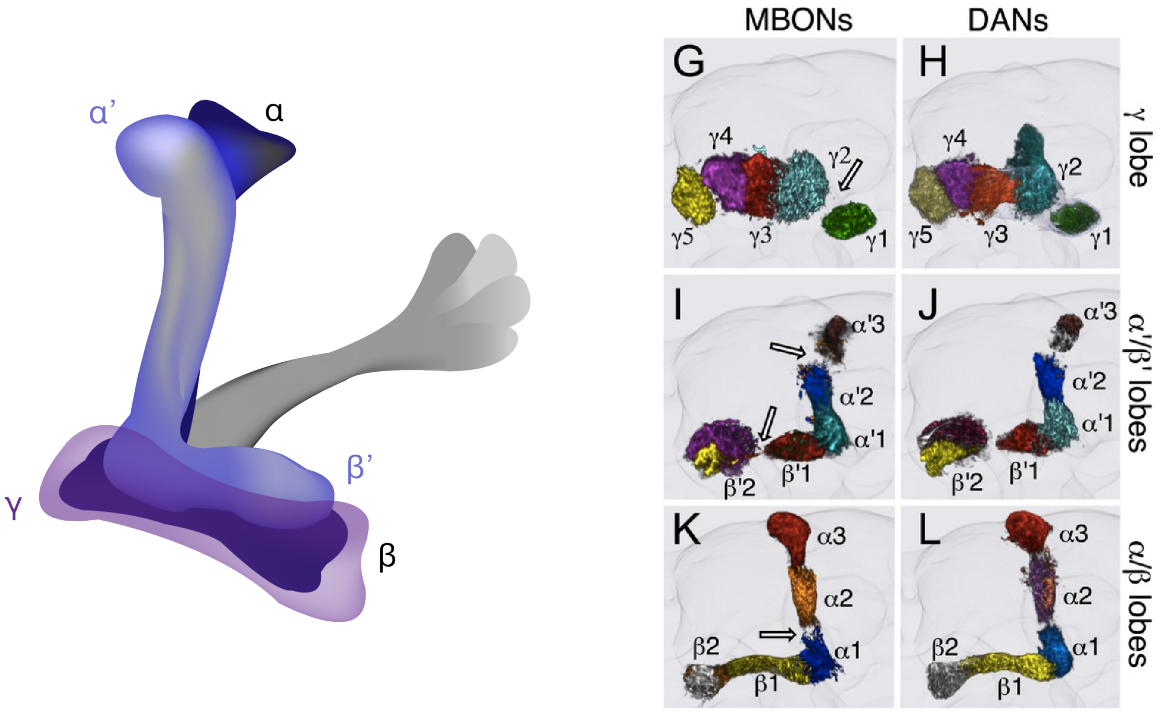

Figure 1.1
Schematic of mushroom body organization. Left: illustration of the mushroom body lobes: the intrinsic cells of the mushroom body (Kenyon cells) are divided into 3 main classes (αβ, navy; α'β', periwinkle; γ, purple), based on their axonal arborizations. Right, G-L originally published in Fig. 10 of (26): The 15 compartments of each MB lobe are defined by the anatomically overlapping dendritic arborizations of mushroom body output neurons (MBONs) (G, I, and K) and axonal aroborizations of dopaminergic neurons (DANs) (H, J, and L). The same false colors were assigned to the DANs and the MBONs of the same compartment. The arrows in (G, I, and K) highlight areas of reduced synaptic density at compartment borders.

Chapter 2

Activation of specific mushroom body output neurons inhibits proboscis extension and feeding behavior

SUMMARY

Animals may become attracted to a previously neutral odor or reject a previously appetitive food source upon learning. In *Drosophila*, the mushroom bodies (MBs) are critical for olfactory associative learning and conditioned taste aversion, but how the output of the MBs affects specific behavioral responses is unresolved. In conditioned taste aversion, *Drosophila* shows a specific behavioral change upon learning, reduced proboscis extension to sugar. While studies have identified MB output neurons (MBONs) that drive approach or avoidance behavior, whether the same or different MBONs impact proboscis extension behavior is unknown. Here, we tested the role of MB pathways in modulating proboscis extension and identified 10 *MBON split-GAL4* lines that upon activation significantly decreased proboscis extension to sugar. Activating several of these lines also decreased sugar consumption, revealing that these MBONs have a general role modifying feeding behavior beyond proboscis extension. Although the MBONs that decreased proboscis extension and ingestion are different from those that drive avoidance behavior in another context, the diversity of their arborizations demonstrates that a distributed network influences proboscis extension behavior. These studies provide insight into how the MB flexibly alters the response to taste compounds and modifies feeding decisions.

INTRODUCTION

A key role of the brain is to prioritize relevant sensory information to guide behavior. Animals exhibit innate behaviors to a variety of sensory stimuli including tastes and odors, and the ability to modify those behaviors based on contextual cues and prior experience is essential to an animal's survival.

In *Drosophila*, the mushroom body (MB) has long been implicated as a center for learning and memory, and has been studied most extensively in the context of olfactory associative learning (18, 19, 67, 68). The dendrites of the principal cells of the MB, Kenyon cells (KCs), receive sparse, random synaptic inputs from olfactory projection neurons. The parallel axonal fibers of the KCs form the MB lobes, the output region of the MB. The ~2000 KC axons of the MB lobes are beautifully organized into 16 compartments, defined anatomically by the dendrites of 22 types of MB output neurons (MBONs). These compartments also contain the axon terminals of 20 types of dopaminergic neurons (DANs), which similarly tile the MB lobes. The DANs convey signals of reward or punishment for sensory associations (18, 29, 30, 32, 69–72). In Pavlovian terminology for a classical conditioning paradigm, the odor is designated the conditioned stimulus (CS), and the DANs carry the unconditioned stimulus (US).

In the current model of olfactory associative learning, behavior is determined through the summation of activity in different MB compartments. Some compartments encode approach behavior, and others encode avoidance (33). In a "naïve" animal, the total valence carried by the positive and negative compartments is in balance, and thus there is no observed approach or avoidance behavior. During olfactory aversive learning, the balance is tipped to favor avoidance behavior: long-term depression is thought to decrease the output in a compartment that signals positive valence (35). Using similar logic, during appetitive olfactory learning, DANs carrying a rewarding signal decrease activity in aversive MBONs, leading to increased acceptance. The sum of synaptic changes drives the overall behavior toward avoidance or acceptance, thereby modifying the innate behavior.

The model described above was developed specifically for olfactory associative learning, and it is not clear how well it generalizes to other learning paradigms. One line of experiments investigated the behavioral roles of MBONs through direct activation (33, 34). Flies expressing a red light-gated channel in the different subsets of MBONs were tested for red light preference or avoidance. Activation of some MBONs caused flies to prefer red light, whereas activation of other MBONs caused flies to avoid red light (33). In addition, activation of some MBON subsets had no discernible effect in this assay. Although these studies support the idea that MBONs can drive approach or avoidance, it is unclear whether MBONs signal a consistently positive or negative valence in the context of different behaviors.

How do the outputs of the MBs influence specific behaviors? One possibility is that MB outputs alter the probability of responding to a given sensory stimulus, independent of the nature of the response. In this model, MB outputs would serve to gate the probability of actions but not participate in action selection. One prediction of this model would be that the MBONs that promote approach might promote other behavioral responses as well. An alternative model is that MBON activity has behavioral specificity. For example, the MBONs that promote approach might be different from the MBONs

that promote ingestion. To begin to examine this question, we tested the role of MB pathways in modulating an innate behavior, proboscis extension to sucrose.

The fly gustatory system is an excellent model to study how MB pathways modulate innate behaviors, as feeding decisions may be altered by learned associations, and importantly, there is a clear behavioral readout: proboscis extension (PER). For example, during conditioned taste aversion, a paired application of sugar to the tarsi and quinine to the proboscis results in a reduced PER to sugar alone (8–11). During conditioned aversion, taste information is transmitted from the subesophageal zone (SEZ) to the MBs for learned associations (11, 63, 73). While studies have found that some components of the MBs are required for taste memory formation, how MBONs impact innate proboscis extension behavior has not been resolved.

In this study, we test the role of MB pathways in modulating PER. We find that a subset of MBONs drives inhibition of proboscis extension. Specifically, we identified 10 *MBON split-Gal4* lines that upon activation significantly decrease proboscis extension to sugar. Inhibiting neural activity in these *MBON split-Gal4* lines did not reciprocally regulate proboscis extension. Activating several of the identified *MBON split-Gal4* lines also decreased sugar consumption, revealing that these MBONs have a more general role in the feeding circuit beyond the proboscis extension motor program. In addition, activating dopaminergic inputs in 3 MB compartments also suppressed proboscis extension to sugar. We also find that the MBONs which decrease proboscis extension to sugar upon activation are not responsive to sucrose. Finally, using *trans*-Tango, we describe some putative areas downstream of the mushroom body that may relay information from the MB to the SEZ, where motor neurons that drive feeding behavior are located. Although the MBONs that decrease proboscis extension and ingestion are different from those mediating avoidance of red light, the diversity of MBON compartments that influences PER demonstrates that a distributed network influences behavior and is consistent with the role of MBs in generating context-dependent behavioral biases.

RESULTS

Activation of MBONs suppresses proboscis extension

To identify the MB outputs that modulate proboscis extension, we screened 35 *split-Gal4* lines that cover the 22 MBON types (33). We crossed the *split-Gal4* lines to *20xUAS-CsChrimson* to generate flies expressing the red-light activated ion channel in MBONs for optogenetic activation experiments. In the fly model, unlike in mammalian systems, dietary supplementation of the all-trans-retinal co-factor is necessary for the production of functional light-gated channels. Flies were raised on standard cornmeal food (controls) or all-trans-retinal-supplemented food (experimental animals) and were starved for 1 day before being tested for proboscis extension. Proboscis extension was tested in response to simultaneous 635 nm light illumination to activate MBONs and 100 mM sucrose presented to the tarsi. For 12 lines, we found that activation with CsChrimson caused a significant decrease in proboscis extension to sucrose (Fig 2.1A).

One line (MB323B) had motor defects and leg folding upon activation and was excluded from further study.

The 11 lines showing reduced proboscis extension upon MBON activation were re-tested for proboscis extension to a range of sucrose concentrations (10, 100, 350, 1000 mM) with and without CsChrimson activation of MBONs. Ten of the 11 lines showed significantly reduced proboscis extension to several sucrose concentrations upon CsChrimson activation (Fig 2.1B). One line (MB062C) did not show a phenotype upon retesting and was excluded from further study (Fig 2.1B). We also repeated the experiment using the red-light-gated channel Chrimson88 and found similar results (Fig S2.1). Importantly, the decrease in proboscis extension was not due to an overall motor defect, as determined by measuring walking speed in a locomotor assay (Fig S2.2). The 10 *MBON split-Gal4* lines that reduced proboscis extension are not localized to any single compartment or lobe. Instead, their neurites arborize in 7 of the 15 mushroom body compartments and the calyx and belong to 7 different MBON cell-types (γ4>γ1γ2, α1, β'1, γ2α'1, α'2, α2sc, and the calyx (Fig 2.1C).

Inhibition of MBON candidates does not influence proboscis extension

As activation of several *MBON split-Gal4* lines decreased proboscis extension to sucrose, we hypothesized that reducing neural activity in those MBONs would cause a reciprocal increase in PER. To test this, we expressed a temperature sensitive, dominant negative dynamin, Shibire^{ts}, using a transgene that drives strong expression (*20xUAS-Shi^{ts1}*) in the 10 *MBON split-Gal4* lines that influenced proboscis extension. Flies were stimulated with 100 mM sucrose applied to the proboscis at 30–32°C to inhibit vesicle reuptake or at ~22°C as same genotype controls. Flies tested at 30–32°C were pre-incubated for 15 minutes prior to the start of the experiment on a 30–32°C heating block. Only one line, MB078C, showed increased PER at the restrictive temperature (Fig 2.2A).

Because the strong Shibire effector has been reported to produce phenotypes at the permissive temperature (33), we repeated these experiments using the weaker *1xUAS-Shi^{ts1}*. We also altered the behavioral paradigm to stimulate with 50 mM sucrose instead of 100 mM sucrose, as PER to 100 mM sucrose under control conditions was high, creating the possibility of ceiling effects. Under these conditions, 1 of the 10 *MBON split-Gal4* lines (MB310C) showed increased proboscis extension upon neural silencing (Fig. 2.2B).

To test if chronic inhibition of the *MBON split-Gal4* lines might influence proboscis extension, we expressed the inward-rectifying potassium channel, Kir2.1, in candidate MBONs. *MBON split-Gal4, UAS-Kir2.1* flies were presented with 30 mM sucrose and proboscis extension was measured and compared to similar genotype controls. One line, MB078C, showed a modest decrease in PER (Fig. 2.2C).

Finally, we tested an additional acute silencing strategy that provides rapid light-triggered hyperpolarization. The light-gated anion channelrhodopsin, gtACR1, was expressed in candidate MBON lines. Flies were stimulated with 10 mM sucrose, as this concentration produced ~50% PER in genotype controls. For each MBON line, the same genotype was examined in the presence of 635 nm light for neural silencing or under control conditions. We found one line (MB242A) where silencing with gtACR1 increases proboscis extension (Fig 2.2D).

Taken all together, the neural silencing experiments argue that the *MBON split-Gal4* lines that inhibited proboscis extension when activated do not consistently alter proboscis extension when inhibited. One explanation may be that proboscis extension to sugar is modulated by MBONs although they are not a required component of the sensorimotor circuit. Instead, the proboscis extension motor program may be controlled by local SEZ circuits and an alternative pathway may relay taste information to the higher brain for learned associations. Alternatively, MBONs may not be intrinsically active and blocking activity in neurons that are already silent may not produce a phenotype. Another possibility is that it may be necessary to silence multiple MBONs in order to produce a phenotype (33). Regardless, these studies demonstrate that inhibiting single classes of MBONs does not strongly influence proboscis extension to sucrose.

Screen for MB DANs regulating PER

In the current model of the MB, activity is balanced between different compartments to drive overall behavior. The dopaminergic inputs to MB compartments are thought to change the strength of synaptic connections between MB neurons and MBONs, mainly through their inputs onto the KCs conveying sensory information (33, 74, 75). Whether those synaptic connections are weakened or strengthened is context-dependent: in some studies DANs appear to inhibit MBON outputs through long term depression (LTD) (26, 34, 35, 76–78), while in other studies DANs have been reported to potentiate KC>MBON connections (34, 79–81). The timing of the DAN and sensory inputs is critically important for determining synaptic potentiation or depression (35, 82).

To investigate whether specific DANs modulate PER and whether they are associated with the same compartments innervated by MBONs that influence PER, we conducted an unbiased screen of DANs. Since activating MBONs innervating γ4>γ1γ2, α1, β'1, γ2α'1, α'2, α2sc, and the calyx suppressed PER, we hypothesized that the DANs innervating those same compartments would cause an increase or decrease in PER.

To conduct the screen, we crossed 33 *DAN split-Gal4* lines to *10x UAS-Chrimson88,* and recorded proboscis extension to sucrose. Flies starved 24 hours were stimulated with 10 mM sucrose presented to the tarsi in the absence (control) or presence of red light to activate DANs and tested for proboscis extension. This sucrose concentration was chosen to provide a range capable of detecting increases or decreases in PER rates. Upon activation with red light, 4 lines showed decreased PER to sucrose (Fig 2.3). Activation of one line (MB438B) caused legs to fold in the red light condition, and was thus excluded from analysis. The remaining DAN lines causing decreased PER mainly innervate the PAM-β'2(amp) and PAM-α1 compartments (as well as weakly PAM-γ5 and PAM-β1).

In addition to these lines whose activation decreased PER, we also found one *DAN split-Gal4* line whose activation caused spontaneous PER: MB296B, a *split-Gal4* for PPL-γ2α’1 (Fig 2.3). We re-tested this line with the effector CsChrimson, and found robust PER to red light (Fig S2.3A). Chronic silencing of these neurons with Kir2.1 resulted in increased PER compared to genetic controls (Fig. S2.3B). Acute silencing with gtACR1 did not have a significant effect (Fig. S2.3C). MB296B labels some neurons outside PPL-γ2α’1 in the SEZ where gustatory sensory axons terminate and proboscis extension motor neurons are located (Fig S2.3D). To address the contribution of non- PPL-γ2α’1 in MB296B, we used an intersectional strategy to restrict CsChrimson

expression to the SEZ using a Hox gene promoter that overlaps with the expression of MB296B (Fig S2.3D). In flies that express the red-light activated channel in the SEZ neurons of MB296B, red light induced PER in some flies (Fig S2.3E), suggesting that the PPL-γ2α'1 neurons are not the causal neurons for this behavior. Since red light caused PER in a subset of flies expressing CsChrimson in the SEZ neurons, it is possible that a combination of the SEZ neurons and the PPL neurons produces a stronger phenotype.

MBON activation also affects sugar consumption

A remaining question is whether MBONs have a more general role in influencing feeding behavior beyond the simple proboscis extension motor program. To address this, we investigated the effect of *MBON split-Gal4* line activation on sucrose consumption. We hypothesized that the set of MBONs whose activation suppresses proboscis extension would also decrease sucrose consumption. In flies starved 24 hours, we measured consumption of 100mM sucrose while activating the 10 *MBON split-Gal4* lines with a PER suppression phenotype using the red-light gated channel 10xChrimson88. Comparing consumption in the presence of red light (for activation) to consumption without red light (controls), we found that 3 lines (MB078C, MB311C, and MB242A) consumed less sugar upon activation (Fig. 2.4). These MBONs provide inputs to the β'1 compartment, the α1 compartment and the MB calyx, respectively.

MBONs do not respond to sucrose

Since activation of MBONs decreases proboscis extension, we considered two possibilities for the mechanism of proboscis suppression. Perhaps MBONs function as a built-in braking mechanism to slow or stop feeding once initiated. In this model, MBONs would be sucrose-responsive, and be part of a negative-feedback motif to ultimately suppress proboscis extension. Alternatively, MBONs are not sucrose-responsive, and another signal must activate the output neurons whose activation suppresses PER. To test the hypothesis that MBONs are sucrose-responsive, we expressed the genetically encoded calcium indicator GCaMP7b in MBONs and used a spinning disc confocal microscope to record responses to sucrose. We did not detect any responses to sucrose in MBONs (Fig.2.5). A subset of PAM-DANs, however, did respond strongly (data not shown.) It is possible that the MBONs respond by hyperpolarizing in response to sugar, but GCaMP is more useful for detecting depolarizations that occur when calcium enters a cell, and does not have the resolution to detect hyperpolarizations well. Greater resolution could be achieved by using a voltage indicator like ArcLight to further test this hypothesis.

***trans*-Tango reveals putative candidates for neurons downstream of MBONs**

To find candidate downstream neurons for the MBONs whose activation cause PER suppression, we used a genetically encoded anterograde tracer, the *trans*-Tango system (83). In the *trans*-Tango system, a ligand (membrane tethered human glucagon) activates a receptor, which triggers proteolytic release of a transcription factor from the plasma membrane and the expression of a target reporter gene. The ligand is attached to Neurexin1 domains, tethering them to the presynaptic membrane. The ligand is only expressed in the neurons of interest (in our case the MBONs), while the receptor and other downstream components are expressed throughout the nervous system. The result is

that the reporter is only activated in cells that are postsynaptic to the starter neurons. During pilot experiments, we noticed some stochasticity in the *trans*-Tango signal (representing putative synaptic partners.) To account for stochasticity and form hypotheses about what neurons are downstream, fly brains were dissected, fixed and stained, then registered to the Janelia common template. The *trans*-Tango signals from these registered brains were then converted to tif files, and the intensity of pixel values (0 to 255) were averaged over several brains using a custom Python script. The average pixel values were saved to a tif image file, and then visualized in FIJI to create a heatmap of likely synaptic partners (Fig. 2.6). In addition to the *trans*-Tango signal, the GFP signal (representing the split-Gal4 expression) was also registered and given the same analysis.

The *trans*-Tango signal for MB077B contained expression localized to the MB, primarily the β'2 compartment. Future work will be required to validate synaptic connections. For the MB-calyx lines (MB242A and MB622B), the *trans*-Tango signal was too saturated, even at 2 weeks with flies reared at 25C (data not shown); future work using younger flies grown at 25°C may restrict expression of the *trans*-Tango signal to fewer neurons and thus give a more useful map of potential downstream partners.

One area that appeared in the *trans*-Tango signal was the fan-shaped body (FB), which was labeled in the *trans*-Tango signal of MB051B, MB078C, and MB080C. As one of the distinct parts of the central complex (84), the FB is reported to be important for multiple functions, including sleep and quiescence regulation (85–87), locomotion (88), visual feature recognition (89) and processing (90), courtship maintenance (91), and regulation of nociceptive avoidance (92).

DISCUSSION

The gustatory system plays a critical role in survival, guiding animals to reject noxious substances and accept nutritious food. Feeding initiation begins with the proboscis extension response (PER), an innate behavior that occurs upon appetitive taste detection. Sensory (47), motor (93, 94), and modulatory (95, 96) neurons for PER all converge in the SEZ, suggesting that local circuits drive this behavior. During aversive taste conditioning, animals learn to avoid an innately appetitive substance, sugar, and no longer show PER to this stimulus. This conditioned behavior requires the mushroom bodies, arguing that MB outputs influence sensorimotor circuits for proboscis extension.

Here we investigate the MBONs that influence proboscis extension and consumption behaviors. Pairing a sucrose stimulus with optogenetic activation of MBONs revealed that 10 MBON split-GAL4 lines reliably decrease PER. In addition, three of the lines linked to decreased PER also decreased sucrose consumption upon activation. None of the MBONs with activation phenotypes had reciprocal phenotypes upon neural silencing. We also examined whether activation of DAN inputs into the MBs influenced PER to sucrose and identified 3 lines that decreased PER (Fig 2.7).

These studies provide data that may inform our larger picture of the way MBONs relate to behavior. The current model of MBON function proposes that each compartment has a positive or negative valence and the combined activity of compartments determines whether the stimulus is attractive or aversive. Consistent with this model, previous

studies have identified MBONs that drive approach and others that drive avoidance. Here, we tested MBONs to see whether they affect PER to sucrose and found that several MBON split-GAL4 lines (MB298B, MB310C, MB311C, MB110C, MB078C, MB051B, MB051C, MB077B, MB080C, MB242A, and MB622B) decreased PER. Of these, MB298B has been implicated in innate avoidance and MB077B has been implicated in innate acceptance, in experiments measuring preference for dark or red-light illuminated quadrants of a chamber in flies expressing CsChrimson under the control of MBON split-GAL4s (26). The other MBONs that decreased PER did not show approach or avoidance behavior upon optogenetic activation in this assay. Additionally, MB080C has been previously described as having a PER suppression phenotype upon activation with UAS-dTrpA1 (11); the other lines identified here were not tested.

The observation that the MBONs that influence PER are different from those that cause innate avoidance argues against a simple model where MBONs have a fixed valence and activity is additive. Instead, these results are consistent with a more nuanced picture in which the role of MBONs in influencing behavior is context-dependent. There are at least three ways in which our study differs from the red-light preference assay: one, flies were starved for 24 hours; two, flies were presented with sucrose; three, the behavioral assay was PER. Both starvation and sucrose detection influence activity in MBs and may alter net MBON activity and the contributions of specific MBONs to behavior. Thus, our results do not distinguish whether different MBONs contribute to different behaviors, (i.e. some MBONs influence approach, some influence PER) or whether different MBONs have different weights in different contexts, (i.e. in starved conditions or in the presence of sucrose). Nevertheless, our studies argue against the notion that MBONs that drive aversion in one context are universersally aversive in all contexts.

The finding that many MBONs reduce the probability of proboscis extension is consistent with the view that the MB is a complex, distributed circuit. The lines with the greatest PER suppression phenotype cover 7 different cell types: γ4>γ1γ2, α1, β'1, γ2α'1, α'2, α2sc, and the calyx, demonstrating that multiple compartments can influence this behavior (Fig. 2.7).

One caveat with these studies is that artificial activation is not physiological and tests the case of strong activation. Under physiological conditions, there are likely more nuanced dynamics that drive behavior. Still, we find strong evidence that multiple MB compartments are able to modulate the drive towards feeding behavior.

Unlike the activation studies, conditional and persistent silencing of MBONs had modest effects on PER in our study, suggesting that there are many parallel pathways or compensatory mechanisms. One possibility is that proboscis extension is mediated by local SEZ circuits and modulated by MBONs. In this scenario, PER circuits may be influenced by MBONs but MBONs do not normally contribute to the behavior. Alternatively, multiple MBONs may contribute to the behavior, consistent with the activation studies, such that silencing a large number of MBONs may be necessary to see a strong phenotype.

We tested whether activation of dopaminergic inputs into the MBs was also sufficient to regulate PER and identified three DAN lines that decreased PER. These innervate the PAM-β'2(amp) and PAM-α1 compartments as well as weakly label PAM-γ5 and PAM-β1. There is no clear correlation between the DAN and MBON

compartments that inhibit PER, since only the α1 compartment contains DANs and MBONs decreasing PER. The DAN activation experiments demonstrate that MB inputs are also sufficient to influence PER but how DAN activation propagates to MBONs to regulate behavior in these experiments is unresolved.

In our studies, the one MB compartment whose activity consistently influenced feeding behavior (both PER and consumption) was α1. The α1 compartment is thought to be important for long-term appetitive memory of nutritious foods (97, 98) and has an unusual circuit structure: its MBON (MBON-α1) appears to form synapses on the dendrites of the DAN that innervates the α1 compartment (PAM-α1), forming a recurrent circuit necessary for long-term memory formation (99). PAM-α1 is also activated by sucrose [unpublished data], so it's interesting that artificially activating PAM-α1 suppresses PER. Since PER is a behavioral readout of how appetitive and rewarding a substance like sugar is, the changes in feeding behavior could be explained by sugar becoming less rewarding under our neuronal activation conditions.

Using calcium imaging, we found that MBONs do not respond to sucrose. These data help to rule out a negative feedback circuit model of feeding modulation where sucrose detection/ feeding activates MBONs, which in turn send signals downstream to put the brakes on feeding. One hypothesis then, would be that MBONs might hyperpolarize in response to sucrose. Follow-up experiments with different tools such as a voltage indicator that allows detection of such events would be informative.

The pathways from the MB to the motor neurons for proboscis extension in the SEZ are still unknown. The results from *trans*-Tango experiments give a glimpse of the areas of the brain that mostly likely receive synaptic inputs. Follow-up experiments would be required to find individual candidate neurons, as these results only provide areas in which to start searching. By comparing these heat maps with the expression patterns of Gal4 drivers in existing databases, we may identify candidate downstream neurons, and then validate connections using functional connectivity (optogenetic activation of the pre-synaptic neuron while recording from the post-synaptic candidate neuron.)

Overall, this work investigates how the activity of MB inputs and outputs impinges on feeding behavior by characterizing mushroom body neurons that impact proboscis extension to sucrose. We demonstrate that activation of several MBONs and DANs influences proboscis extension to sucrose, consistent with distributed network of MB compartments involved in driving a behavior.

MATERIALS AND METHODS

Fly stocks

The following fly lines were used:
MBON split-Gal4 lines (26);
20xUAS-CsChrimson-mVenus (attP18) (100);
10xUAS-Chrimson88-tdTomato3.1 (attp18) (David Anderson lab);
UAS-Shibire^{ts} (101);
20xUAS-Shibire^{ts} (102);
20xUAS-gtACR1 (103);

*UAS-Kir2.*1 (104);
DAN split-Gal4 lines (26);
w^{1118}; pBPp65ADZpUw (attP40) ; pBPZpGAL4DBDUw (attP2) ("EmptySplit") (105);
20xUAS-dsFRT-CsChrimson-mVenus (106);
LexAop-FLP (107);
scr-LexA (108)
UAS-myr-GFP, QUAS-tdTomato (attp8); *trans-Tango*(attp40) (83);
w1118; 20XUAS-IVS-jGCaMP7b (VK00005) (109)

Drosophila stocks were maintained at 25°C except those containing temperature-sensitive transgenes (*Shibire^{ts}*) which were raised at 19°C. Flies were reared on standard fly food, except in experiments involving CsChrimson, Chrimson88, and gtACR1, which were transferred to food containing 0.4mM retinal prior to experiments.

Behavior

Behavioral assays were done using mated female flies, 4-9 days post-eclosion. All animals were starved for 20-26 hours in a vial containing a wet kimwipe with 3 mL double distilled water.

For optogenetic experiments, flies with *UAS-Chrimson88*, *UAS-CsChrimson*, or *UAS-gtACR1* transgenes were raised in the dark at 25°C. Two days prior to behavioral testing, flies were transferred to fresh food containing 0.4 mM all-trans retinal (Sigma). Flies were then starved on a wet kimwipe with the same retinal concentration. For activation experiments (CsChrimson, Chrimson88), flies were assayed one at a time with 635 nm light (LaserGlow). Silencing with gtACR1 was done using a custom-built LED panel (530nm) or 530-535nm laser (LaserGlow). For 1xShibire^{ts} and 20xShibire^{ts} experiments, flies were reared at either 19°C or 23°C. During the experiment, mounted flies were incubated at 30–32°C on a heating block for 15 minutes prior to the start of and throughout the experiment. For Kir2.1 experiments, flies were reared at 25°C.

Proboscis Extension Response Assays

PER was performed as previously described (96), except that each animal was treated as an independent data point. Briefly, flies were mounted on glass microscope slides with either nail polish or UV glue (12 flies per slide for optogenetic experiments, and 36 flies per slide for Kir2.1 and Shibire experiments), and then allowed to recover for 15 minutes before being placed in a dark, humidified chamber for 2-5 hours. Prior to testing and between trials, flies were allowed to drink water ad libitum.

In the CsChrimson screen, we simultaneously activated the MBONs while presenting 100 mM sucrose to the tarsi. This concentration was chosen because it is a moderately appetitive stimulus that results in proboscis extension ~50% of the time in control flies. Flies were water-satiated before the experiment and between trials, and presented with the tastant and red light until a proboscis extension was observed, for up to 5 seconds. Flies were given a score of 0 (for no extension) or 1 (for full extension), and the average was taken across two trials.

For thermogenetic silencing experiments (20xShibire^{ts} and 1xShibire^{ts}), flies were assayed with 100 mM sucrose and 50 mM sucrose, respectively. For Kir2.1 experiments, flies were presented 30 mM sucrose.

For all subsequent optogenetic (Chrimson88, gtACR1) PER assays with both MBONs and DANs, flies were assayed using 10 mM sucrose because 50 mM sucrose elicited close to 100% PER in the dark condition for some lines.

Temporal Consumption Assays

Temporal consumption assays were performed as previously described (73). Briefly, flies were glued onto glass slides using nail polish or UV glue, then allowed to recover in a humidified chamber for 2-4 hours. Each fly was water-satiated, then presented with 100 mM sucrose on the proboscis and forelegs. Cumulative drinking time over 10 consecutive presentations was recorded.

Immunohistochemistry

Dissection and immunohistochemistry of fly brains were performed using the Janelia *split-Gal4* screen protocol (https://www.janelia.org/project-team/flylight/protocols) with small modifications. Briefly, brains and VNCs of (23- to 60- day-old for *trans*-Tango experiments or 9- to 14- day old for all other experiments) female flies were dissected in Schneider's insect medium and fixed in 2% paraformaldehyde in Schneider's medium for 60 min at room temperature. After washing in PBT (0.5% Triton X-100 in PBS) twice for 10-15 minutes each, tissues were dipped in PBS to remove the Triton, then mounted onto a poly-L-lysine coated glass coverslip. Tissues were then were blocked in 5% normal goat serum for 90 min. After blocking, tissues were incubated in primary antibodies diluted in 5% serum in PBT for 3–7 days on a nutator at 4°C, washed three times in PBT for 30 min or longer, then incubated in secondary antibodies diluted in 5% serum in PBT for 3–7 days on a nutator at 4°C. Afterwards, tissues were washed in PBT 4 times for at least 30 minutes each, before dehydration and clearing (see below).

Tissues were incubated in mixtures of multiple primary or secondary antibodies in Coplin jars. The following primary antibodies were used: chicken anti-GFP (Life Technologies, 1:500) and mouse anti-nc82 (Developmental Studies Hybridoma Bank, Iowa City, IA 1:500). The following secondary antibodies were used (both Invitrogen at 1:100): 488 anti-chicken, 647 anti-mouse.

After immunohistochemistry, tissues were dehydrated through a series of ethanol baths (30%, 50%, 75%, 95%, and 3 × 100%) for 10 min each and then cleared using 100% xylene three times for 5 minutes each. Samples were embedded in a xylene-based mounting medium (DPX; Electron Microscopy Sciences, Hatfield, PA), and the DPX was allowed to dry for at least 24 hours before imaging. All images were acquired on a Zeiss confocal microscope. Brightness and contrast were adjusted using FIJI.

Locomotor Assay

Flies were gently aspirated into a circular bowl chamber made of 1.5% agarose, 44 mm in diameter [Bidaye et al., unpublished]. The stimulation protocol was 60s off, 30s pulsing 633nm light at 50 Hz. Light was delivered using a custom LED panel. Freely moving flies were videotaped under IR illumination using a Blackfly camera. The movie was subsequently analyzed using the Ctrax software suite version 0.3.9 (110). The total distance walked was computed and used to generate a mean distance traveled for each genotype assayed.

trans-Tango Data Analysis

UAS-myr-GFP, QUAS-tdTomato (attp8); *trans-Tango* (attp40) were crossed to *MBON-splitGal4* lines. Flies were reared at 19°C and aged 30-60 days to allow for maximal expression of the trans-Tango signal. Mated female flies were dissected and treated as described above (Immunohistochemistry.) Brains were scanned with a Zeiss confocal microscope. Stacks were then registered to a common template using the CMTK registration pipeline. These registered brains were analyzed using python. Briefly, each image was normalized to the maximum pixel intensity of each image, and then the average pixel value across all flies of each genotype was plotted, to create a heatmap of likely synaptic partners of the MBONs. Images were adjusted in FIJI.

Calcium imaging

Calcium transients were imaged in flies expressing one copy of *20xUAS-GCaMP7b* on a fixed-stage 3i spinning disk confocal microscope with a piezo drive and a 20x water objective (1.6x optical zoom), using a modified version of previously described in vivo preparation as previously described (63, 111). Briefly, fly heads were secured with UV glue on the optic lobes instead of nail polish, the esophagus was left intact. The brain immersed in AHL as previously described, while the taste organs remained dry and accessible for stimulation with natural taste stimuli.

Flies were stimulated with 1M sucrose to the proboscis, while the MB was imaged. The proboscis was waxed out, the antennae were removed, and the dorsal cuticle and underlying air sacs were removed. Sucrose was presented to the proboscis via capillary tube (9).

GCaMP7b, with its high baseline fluorescence levels, was used to define the imaging volume and fast z-sectioning with a piezo drive allowed for volumetric 4D imaging. Calcium signal was imaged with a 488 nm laser with 100ms exposure. Sucrose was presented at time points 10-12 and 20-22, and then 1M KCl was delivered via a pipette at time point 30. Forty or 50 total time points were acquired; 40 timepoints were plotted during analysis.

For every fly, Z-slices containing dendrites, and when visible, soma, were selected for imaging and analysis. A max projection across z for the anatomy scan and each GCaMP time point was used for analysis. An ROI containing the neuronal region were drawn by hand. In addition, an ROI was drawn in a region that did not express GCaMP to measure background autofluorescence. Mean fluorescence levels from the background ROI were subtracted from the anatomical ROI at each timepoint, to give the change in fluorescence over time: F(t). $\Delta F/F$ was calculated as $[F(t) - F_0]/ F_0$, where F_0 is the average fluorescence for the 4 time points preceding the first stimulation. ROI drawing and fluorescence measures were done in FIJI. Analysis and plotting of calcium transients was done using R.

Statistical Analyses

Statistical analyses were done using R (ggPubR). For PER in response to red light and sucrose in the CsChrimson screen, Wilcoxon rank-sum tests with Bonferroni correction for multiple comparisons were used to compare the PER rate in retinal-exposed vs. no-retinal animals. For all other optogenetic PER assays, paired Wilcoxon

tests with Bonferroni correction were used, since individual animals were tested both in the dark and light conditions. For PER experiments with Shi^{ts1}, unpaired Wilcoxon tests were used since different populations of genetically identical animals were tested at the permissive room temperature (22°) and the restrictive temperature (32°). For TCA experiments, Wilcoxon rank-sum tests were used with Bonferroni correction for multiple comparisons.

Figure 2.1

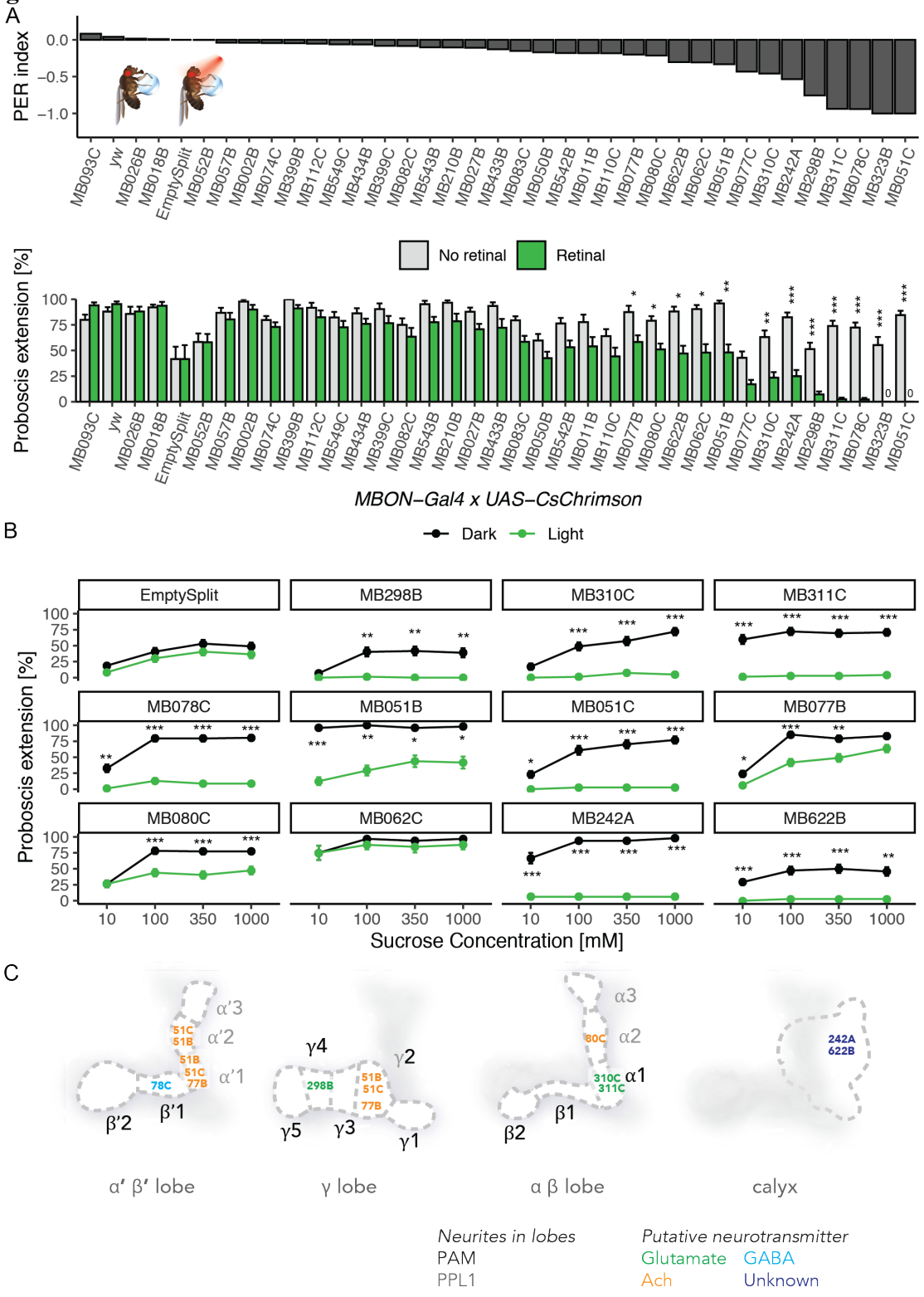
A
PER index
0.0
−0.5
−1.0
MB093C yw MB026B MB018B EmptySplit MB052B MB057B MB002B MB074C MB399B MB112C MB549C MB434B MB399C MB082C MB543B MB210B MB027B MB433B MB083C MB050B MB542B MB011B MB110C MB077B MB080C MB622B MB062C MB051B MB077C MB310C MB242A MB298B MB311C MB078C MB323B MB051C
No retinal
Retinal
Proboscis extension [%]
100
75
50
25
0
MB093C yw MB026B MB018B EmptySplit MB052B MB057B MB002B MB074C MB399B MB112C MB549C MB434B MB399C MB082C MB543B MB210B MB027B MB433B MB083C MB050B MB542B MB011B MB110C MB077B MB080C MB622B MB062C MB051B MB077C MB310C MB242A MB298B MB311C MB078C MB323B MB051C
MBON−Gal4 x UAS−CsChrimson
B
Dark
Light
EmptySplit
MB298B
MB310C
MB311C
MB078C
MB051B
MB051C
MB077B
MB080C
MB062C
MB242A
MB622B
Proboscis extension [%]
10 100 350 1000
Sucrose Concentration [mM]
C
α'3
α'2
α'1
β'2
β'1
51C
51B
78C
77B
γ4
γ2
γ5
γ3
γ1
298B
α3
α2
α1
β1
β2
80C
310C
311C
242A
622B
α' β' lobe
γ lobe
α β lobe
calyx
Neurites in lobes
PAM
PPL1
Putative neurotransmitter
Glutamate
GABA
Ach
Unknown

Figure 2.1. Identification of MBONs that suppress proboscis extension to sucrose
A) Behavioral screen for flies that change their rate of proboscis extension when MBONs are activated. *MBON split-Gal4* lines were crossed to *UAS-CsChrimson* for light induced activation, and tested for proboscis extension to simultaneous red light and sucrose presentation to the tarsi. Extension rates were compared between flies fed retinal and those not. (n = 20-48 flies per line). Inset: Illustration of the PER assay. Top: results of the screen, ordered by PER index to reveal Gal4 lines with the greatest change in PER upon MBON activation. PER index = (Retinal – no retinal) / (Retinal + no retinal). Bottom: Same data ordered as in top, shown as mean ± SEM. Statistical significance was calculated using Wilcoxon Rank Sum tests (retinal versus no retinal) with Bonferroni correction for multiple comparisons, *$p<0.05$, **$p < 0.01$, ***$p < 0.001$. Green bars represent flies fed retinal. Grey bars represent flies not fed retinal. B) Retest of candidates causing the greatest PER suppression upon MBON activation with CsChrimson. Values represent mean (± SEM) fraction of flies presented with sucrose (black lines) and flies presented with sucrose and red light (green lines) exhibiting PER to the indicated concentrations of sucrose (n = 26-57). Asterisks denote statistically significant differences between flies in light and dark conditions. Statistical significance was calculated using a two-way ANOVA with Bonferroni correction, where *$p<0.05$, **$p < 0.01$, ***$p < 0.001$. C) Schematic of dendritic arborizations of the *MBON split-Gal4* lines that caused the greatest PER suppression phenotypes in the activation screen. Each lobe of the MB, as well as the calyx, is drawn separately for visual clarity. The name of each *MBON split-Gal4* is spatially localized to the compartments where it has dendritic arborizations. Colors indicate putative neurotransmitters for MBONs and cluster of origin for DANs.

Figure S2.1

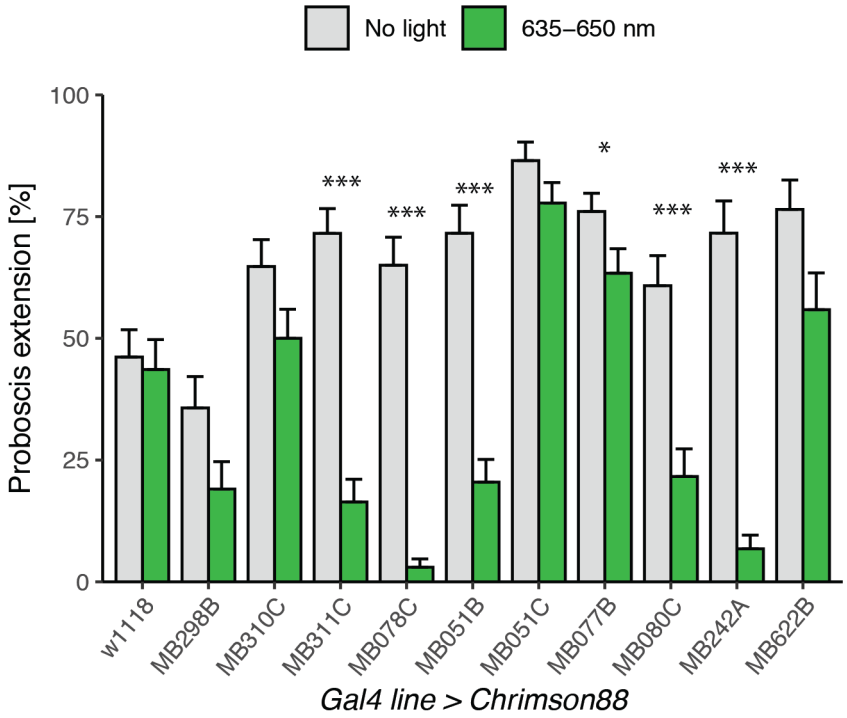

Figure S2.1. Supplemental to Figure 1. Retest of flies that change proboscis extension rate when MBONs are activated, using *UAS-Chrimson88*
MBON split-Gal4 lines were crossed to *UAS-Chrimson88* for light induced activation, and tested for proboscis extension to tarsal sucrose presentation, followed by simultaneous red light and sucrose presentation to the tarsi. Extension rates were compared between light and dark conditions in the same fly (n = 34-71 flies per line). Values represent mean ± SEM. Statistical significance was calculated using paired Wilcoxon Rank Sum tests (light versus no light) with Bonferroni correction for multiple comparisons, **p < 0.01, ***p < 0.001. Green bars represent flies given sucrose and red light. Grey bars represent extensions to sucrose without red light.

Figure S2.2

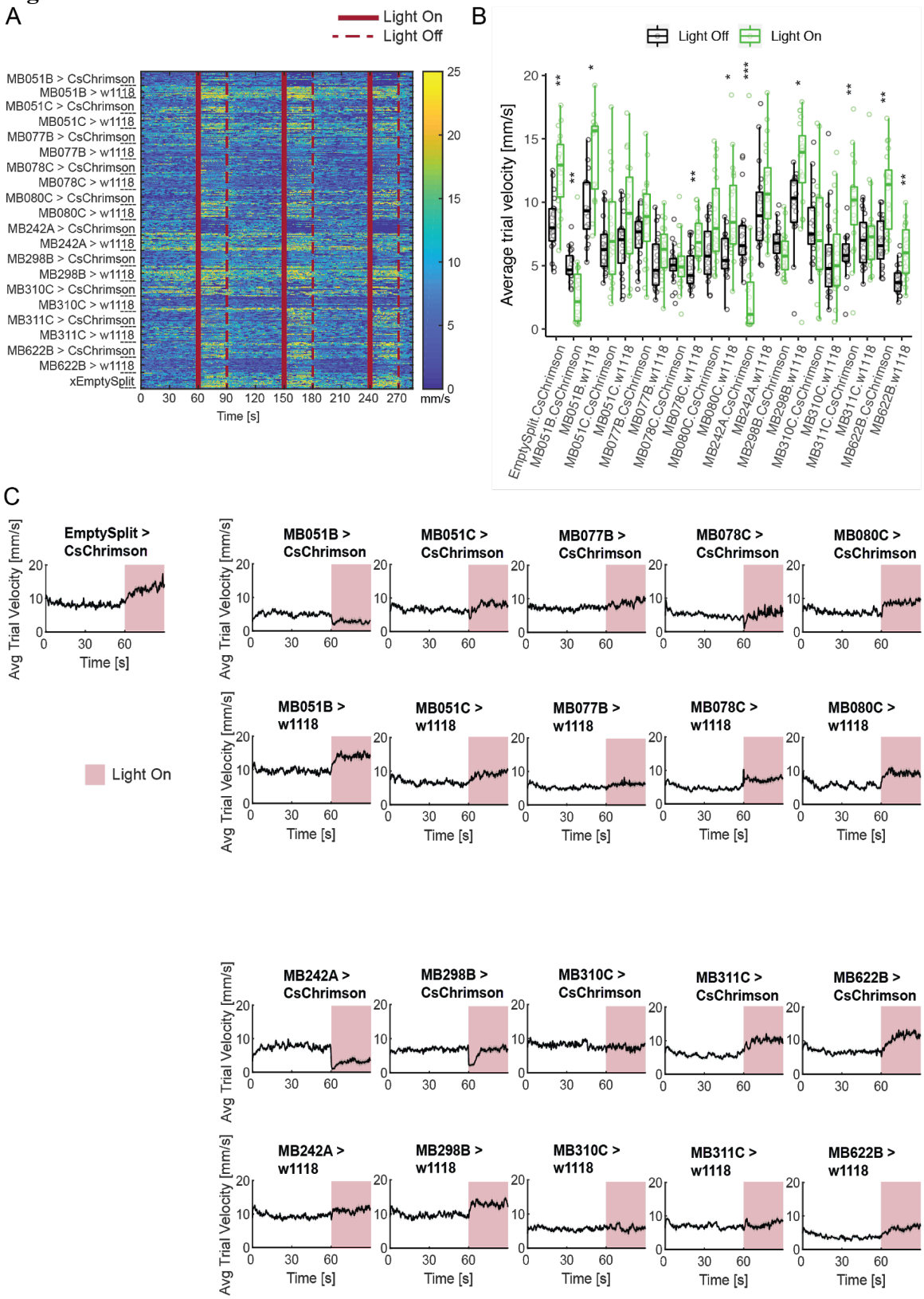
A
Light On
Light Off
MB051B > CsChrimson
MB051B > w1118
MB051C > CsChrimson
MB051C > w1118
MB077B > CsChrimson
MB077B > w1118
MB078C > CsChrimson
MB078C > w1118
MB080C > CsChrimson
MB080C > w1118
MB242A > CsChrimson
MB242A > w1118
MB298B > CsChrimson
MB298B > w1118
MB310C > CsChrimson
MB310C > w1118
MB311C > CsChrimson
MB311C > w1118
MB622B > CsChrimson
MB622B > w1118
xEmptySplit
0 30 60 90 120 150 180 210 240 270
Time [s]
25 20 15 10 5 0
mm/s
B
Light Off
Light On
Average trial velocity [mm/s]
20 15 10 5 0
EmptySplit.CsChrimson
MB051B.CsChrimson
MB051B.w1118
MB051C.CsChrimson
MB051C.w1118
MB077B.CsChrimson
MB077B.w1118
MB078C.CsChrimson
MB078C.w1118
MB080C.CsChrimson
MB080C.w1118
MB242A.CsChrimson
MB242A.w1118
MB298B.CsChrimson
MB298B.w1118
MB310C.CsChrimson
MB310C.w1118
MB311C.CsChrimson
MB311C.w1118
MB622B.CsChrimson
MB622B.w1118
C
EmptySplit > CsChrimson
MB051B > CsChrimson
MB051C > CsChrimson
MB077B > CsChrimson
MB078C > CsChrimson
MB080C > CsChrimson
MB051B > w1118
MB051C > w1118
MB077B > w1118
MB078C > w1118
MB080C > w1118
MB242A > CsChrimson
MB298B > CsChrimson
MB310C > CsChrimson
MB311C > CsChrimson
MB622B > CsChrimson
MB242A > w1118
MB298B > w1118
MB310C > w1118
MB311C > w1118
MB622B > w1118
Avg Trial Velocity [mm/s]
Time [s]
Light On

Figure S2.2. Supplement to Figure 1. Locomotor assay. *MBON split-Gal4* lines were crossed to *UAS-CsChrimson*, as well as w^{1118} (controls). Single flies were placed in a circular agar bowl arena. Fly position was tracked under IR illumination with a camera, and then subsequently analyzed using ctrax and custom matlab scripts. The stimulation protocol was 3x (60s off, 30s on pulsing 633nm light at 50 Hz), and a total of 5 minutes of video was recorded for each trial. A) Heat map of velocities, each row is an individual fly. Genotypes are denoted. B) Box and whiskers plot of average velocity over 3 trials, for light off and light on periods. Each data point is one fly, whiskers = 10th to 90th percentile, box = 25th to 75th percentile, and line in box = median. Statistical significance was calculated using paired Wilcoxon Rank Sum tests (light off vs. light on) with Bonferroni correction for multiple comparisons, * $p<0.05$, ** $p < 0.01$, *** $p < 0.001$. Black represents flies in the light off period. Green represent flies in the red-light on period. C) Bounded line plots. For each fly, the average velocity over 3 trials of (60s Light Off, 30s Light On) was calculated. The black line represents the mean average trial velocities of n = 16-20 flies for each genotype; the shaded grey areas represent the standard error. *MBON split-Gal4* lines crossed with *UAS-CsChrimson* are on top, paired with the genetic controls of *MBON split-Gal4* lines crossed with w^{1118}, bottom. The red box denotes the light on period, starting at 60s.

Figure 2.2

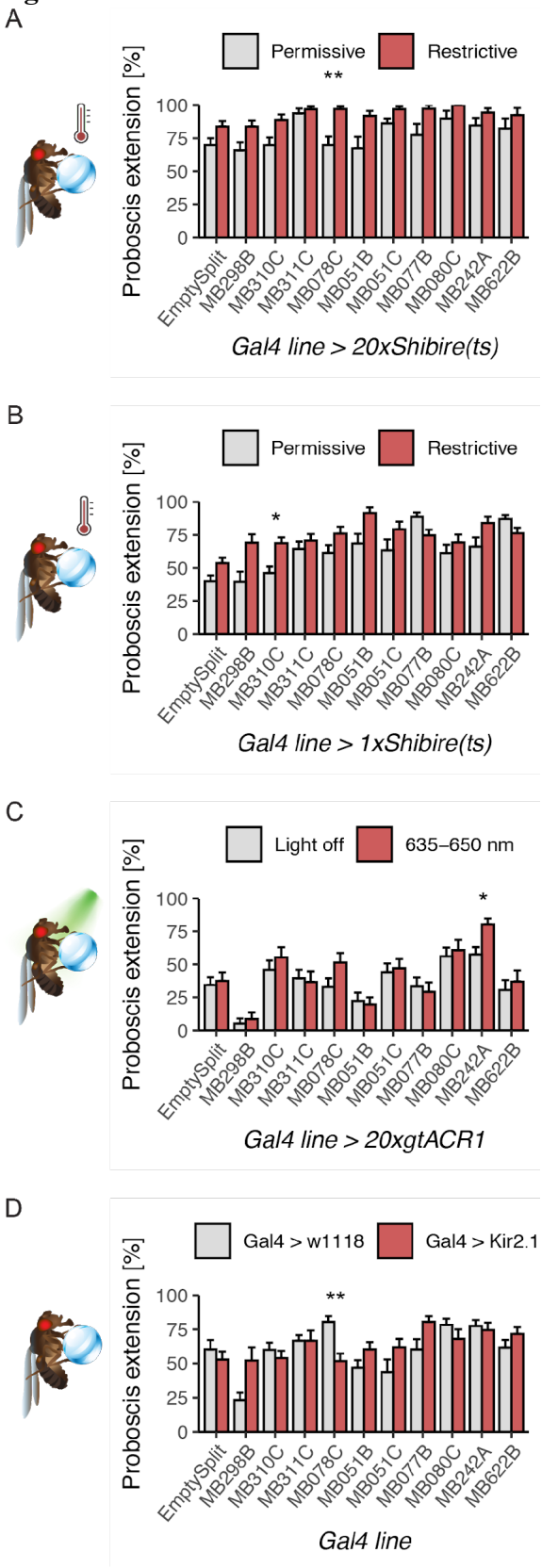
A
Permissive
Restrictive
**
Proboscis extension [%]
100
75
50
25
0
EmptySplit
MB298B
MB310C
MB311C
MB078C
MB051B
MB051C
MB077B
MB080C
MB242A
MB622B
Gal4 line > 20xShibire(ts)
B
Permissive
Restrictive
*
Proboscis extension [%]
Gal4 line > 1xShibire(ts)
C
Light off
635–650 nm
*
Proboscis extension [%]
Gal4 line > 20xgtACR1
D
Gal4 > w1118
Gal4 > Kir2.1
**
Proboscis extension [%]
Gal4 line

Figure 2.2 Decreasing neural activity in MBONs that suppress PER when activated has modest effects

A) MBON lines identified in our activation screen were conditionally silenced with 20xShibire^{ts} and PER to tarsal sugar presentation (100 mM sucrose) was recorded. n = 18-59. Permissive temperature= 20-22°C, restrictive = 30–32°C. B) MBON candidates were conditionally silenced with 1xShibire^{ts} and PER to 50 mM sucrose on the legs was recorded. Silencing MBONs with this method caused an increase in PER rate in one line (MB310C). n = 20-74 C) Candidates were silenced acutely with the light-gated anion channelrhodopsin 20xgtACR1 and PER to 10 mM sucrose on the legs was recorded. Silencing MBONs with this method resulted in increased PER in one line (MB242A). n = 16-36. D) Candidates were inhibited with Kir2.1 and PER to 30 mM sucrose on the legs was recorded. Silencing MBONs with this method caused a decrease in PER rate in one line (MB078C). n = 18-60. For all graphs, error bars indicate mean ± SEM. Statistical significance was determined by Wilcoxon Rank Sum tests with Bonferroni correction for multiple comparisons, *$p<0.05$, **$p<0.01$.

Figure 2.3

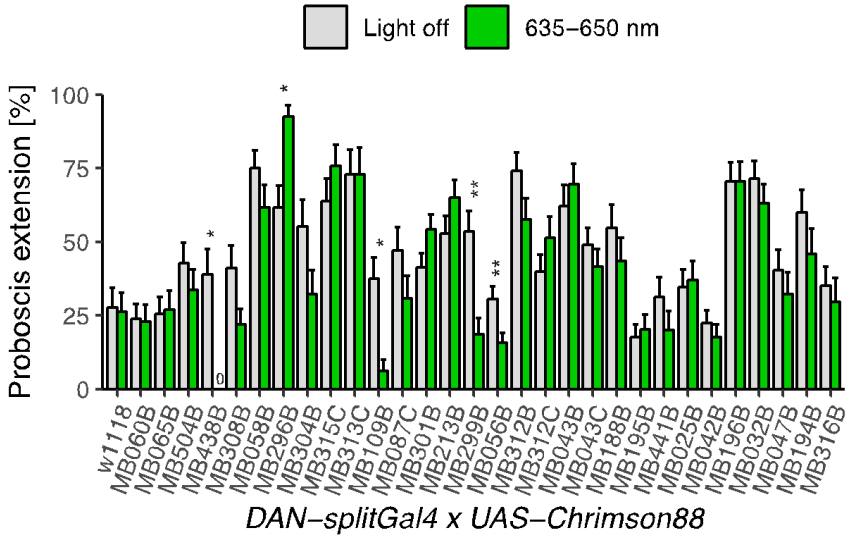

Figure 2.3. Identification of DANs that modulate PER to sucrose
Behavioral screen for flies that change proboscis extension rate when DANs are activated. *DAN split-Gal4* lines were crossed to *UAS-Chrimson88* for light induced activation, and tested for proboscis extension to 10 mM sucrose presentation to the tarsi, and then simultaneous sucrose presentation to the tarsi and red laser light. Extension rates were compared between light and dark conditions in the same fly (n = 24-81 flies per line). Values represent mean ± SEM. Statistical significance was calculated using paired Wilcoxon Rank Sum tests (light versus no light) with Bonferroni correction for multiple comparisons, *$p < 0.05$, **$p < 0.01$.

Figure S2.3.

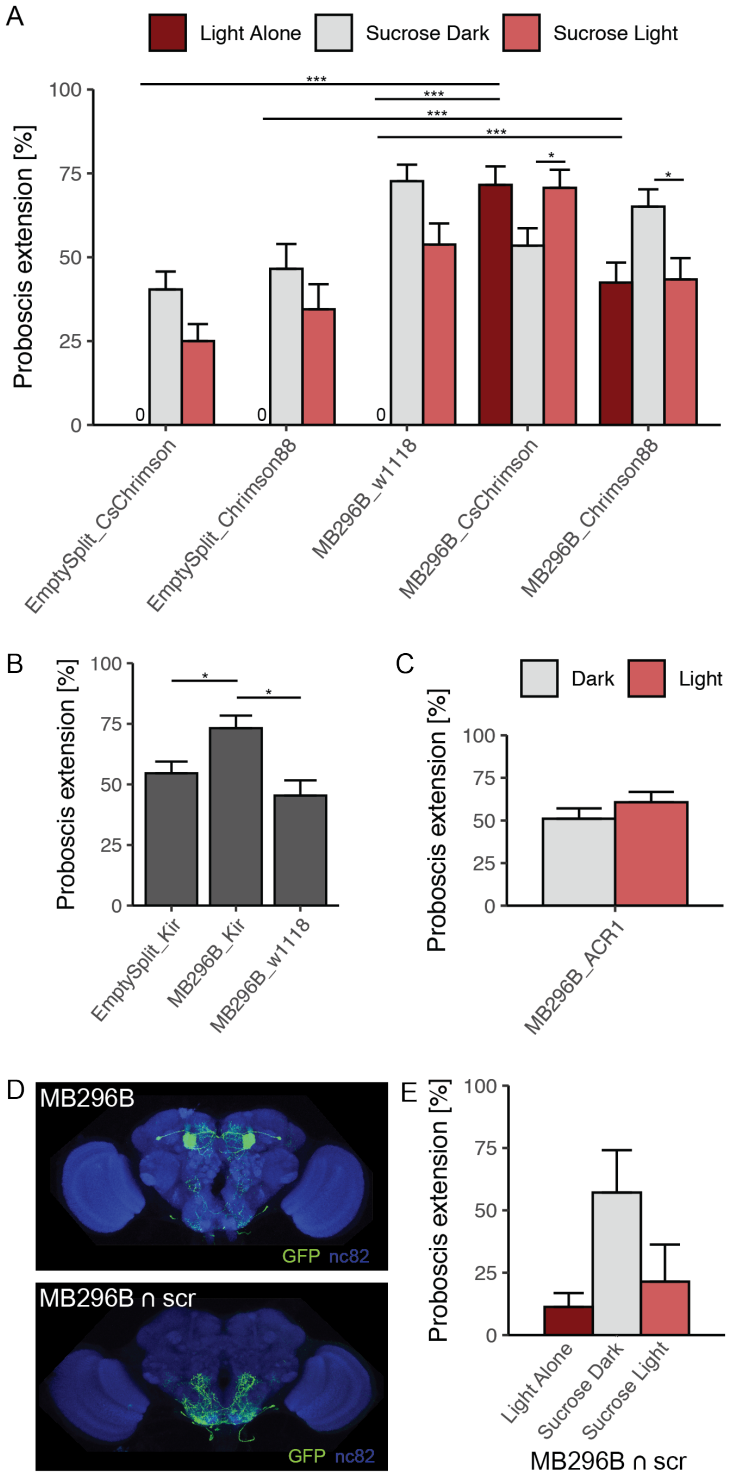
A
Light Alone
Sucrose Dark
Sucrose Light
Proboscis extension [%]
EmptySplit_CsChrimson
EmptySplit_Chrimson88
MB296B_w1118
MB296B_CsChrimson
MB296B_Chrimson88
B
EmptySplit_Kir
MB296B_Kir
MB296B_w1118
C
Dark
Light
MB296B_ACR1
D
MB296B
GFP nc82
MB296B ∩ scr
GFP nc82
E
Light Alone
Sucrose Dark
Sucrose Light
MB296B ∩ scr

Figure S2.3. Activation of he SEZ neuron labeled by MB296B causes PER.
A) *MB296B split-Gal4* was crossed to *UAS-Chrimson88* and *UAS-CsChrimson* for light induced activation, and tested for proboscis extension in 3 conditions: (1) red light alone, (2) 30 mM sucrose to the tarsi, and (3) simultaneous red light and sucrose presentation to the tarsi. Extension rates were compared between each condition in the same fly, and between different fly genotypes of the same condition for genetic controls (n = 27-58 flies). Values represent mean ± SEM. Statistical significance was calculated using paired Wilcoxon Rank Sum tests (between different conditions of the same flies) or unpaired Wilcoxon Rank Sum tests (between flies of different genotypes in the same treatment condition) with Bonferroni correction for multiple comparisons, *$p < 0.05$, ***$p < 0.001$. Green bars represent flies given sucrose and red light. Grey bars represent extensions to sucrose without red light. B) MB296B was inhibited with Kir2.1 and PER to 30 mM sucrose on the legs was recorded. Silencing with Kir2.1 resulted in increased PER (n = 44-56). Error bars indicate mean ± SEM. Statistical significance was determined by Wilcoxon rank sum tests with Bonferroni correction for multiple comparisons, *$p<0.05$. C) Candidates were silenced with 20xgtACR1 and PER to 30 mM sucrose on the legs was recorded, in the absence and presence of green light. Silencing MB296B with this method did not cause statistically significant changes in PER rate. n = 47. Error bars indicate mean ± SEM. Statistical significance was determined by a paired Wilcoxon test. D) Top: Projection pattern of MB296B. Bottom: Projection pattern of the SEZ neuron labeled by MB296B, as determined by an intersection between the Hox gene scr and MB296B. E) *MB296B-split-Gal4* was crossed to *20xUAS-dsFRT-CsChrimson.mVenus*; *LexAop-FLP*/*CyO*; *scr-LexA*/*TM2* flies for light induced activation, and tested for proboscis extension to light (n = 31.) Of these 31 flies, 7 were also tested for their responses to 30 mM sucrose to the tarsi, and simultaneous red light and sucrose presentation to the tarsi as well.

Figure 2.4

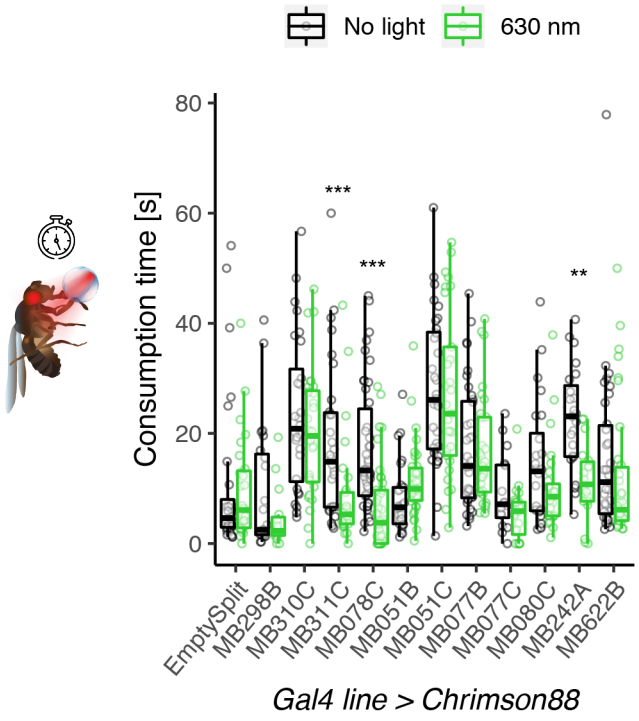

Figure 2.4. Activation of MBONs causes a reduction in sucrose consumption
Activation of 3 *MBON split-Gal4* lines (MB311C, MB078C, MB242A) using Chrimson88 caused decreased consumption of 100 mM sucrose. Box and whiskers plot shows fed light and no light conditions; each data point represents one fly; whiskers = 10th to 90th percentile, box = 25th to 75th percentile, and line in box = median. Statistical significance was calculated using paired Wilcoxon Rank Sum tests (light versus no light) with Bonferroni correction for multiple comparisons; **p<0.01, ***p<0.001; n = 15-42 flies per line.

Figure 2.5

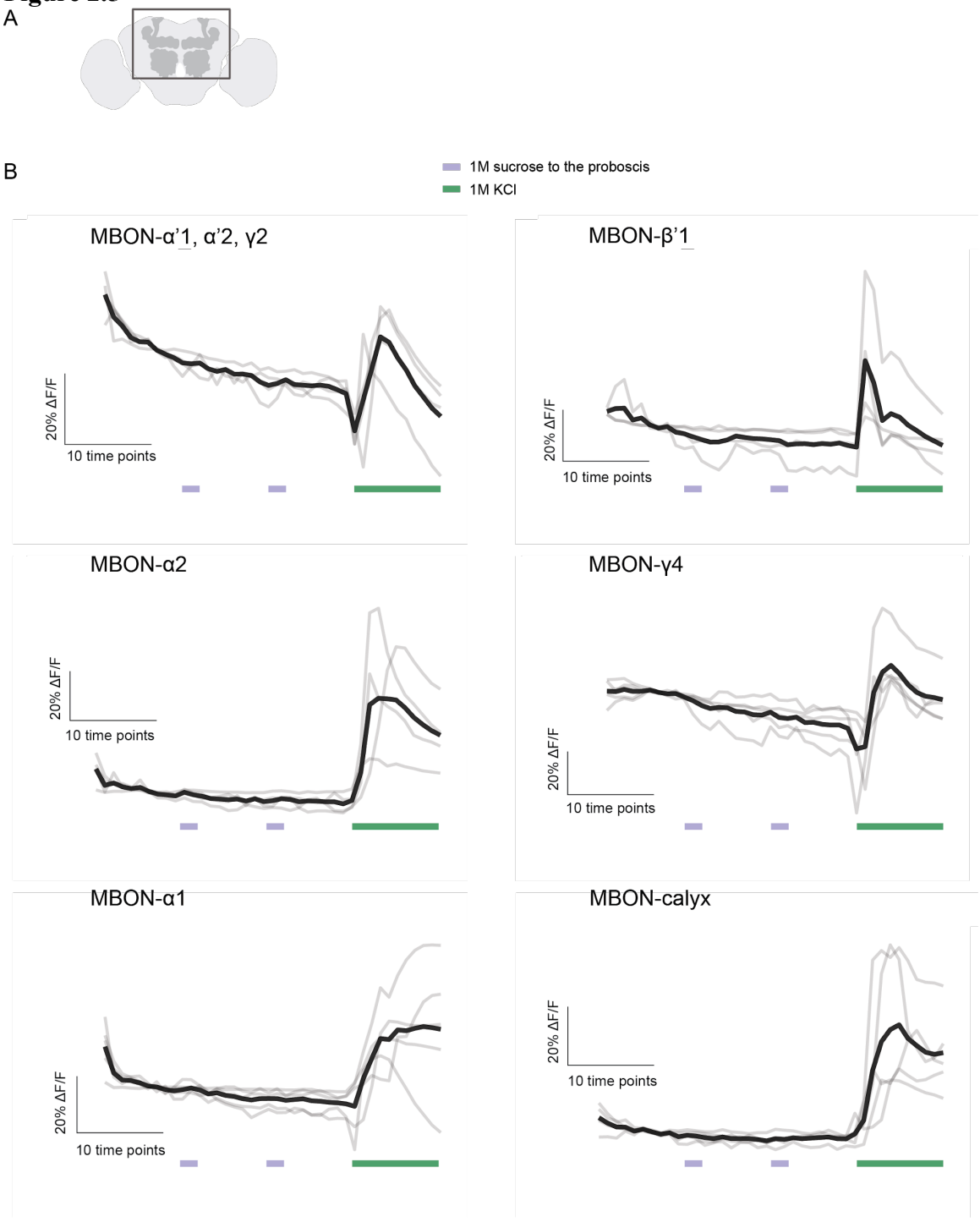

Figure 2.5. MBONs do not respond to sucrose. (A) Schematic showing the approximate region of imaging (black box). (B) ΔF/F traces, each grey line is one fly, black line represents the mean ΔF/F trace per genotype. 1M sucrose (purple) was presented to the proboscis of the fly at frames 10-12 and frames 20-22. 1M KCl (green) was delivered at time point 30.

Figure 2.6

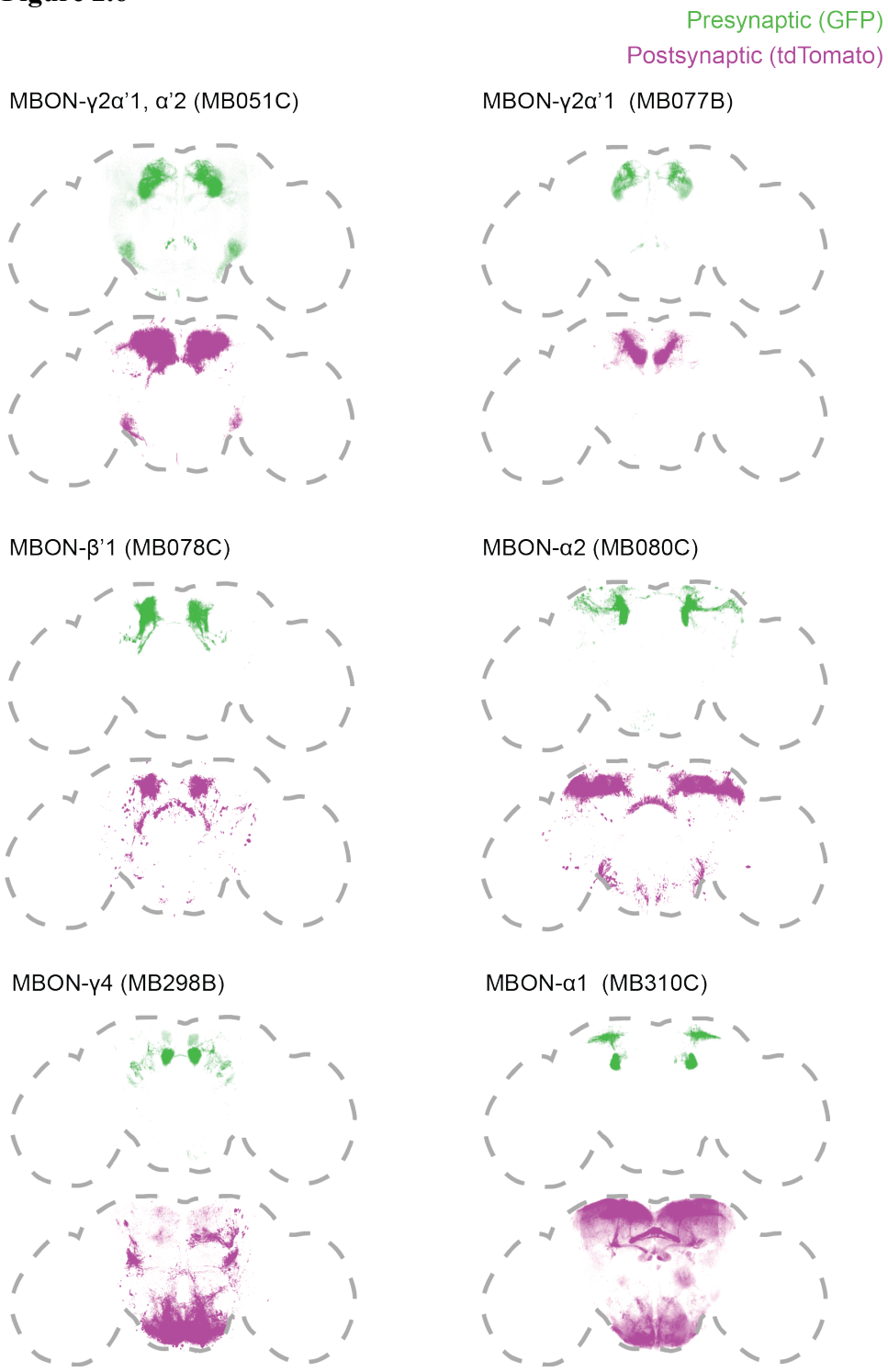

Figure 2.6. *trans*-Tango signals reveal putative downstream synaptic partners of MBONs that suppress PER when activated. Each image represents the averaged sum of signals from registered brains. Top is GFP signal in green; Bottom is the *trans*-Tango tdTomato signal in magenta. (n = 5-13 per genotype)

Figure 2.7.

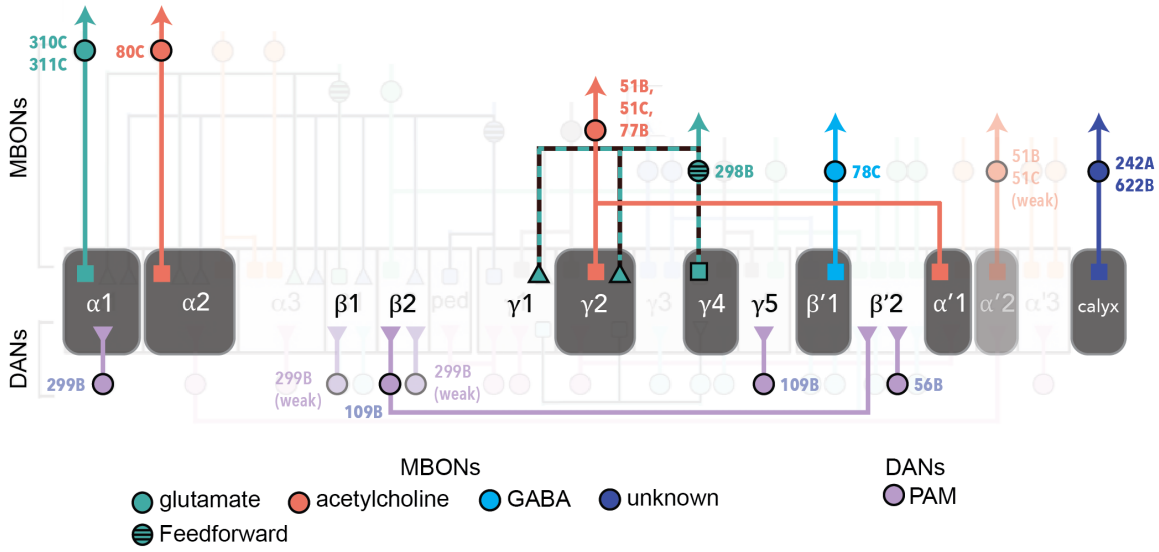

Figure 2.7. Schematic summary of MBONs and DANs whose activity influence PER Schematic of the MB circuits of DAN inputs (bottom) and MBON outputs (top) whose activity influences PER. The 7 MB lobe compartments where MBON activation suppresses PER are shown in the grey rectangles (middle). Dendritic arborizations are represented by squares; triangles represent axonal arborizations. Each MBON-Gal4 is color-coded to show its putative neurotransmitter. The cluster of origin of the dopaminergic inputs for each compartment is also indicated by the color of the compartment label. MB051B, MB051C, and MB077B contain dendrites in 2 compartments. One MBON, MB298B, illustrated with a dashed line and striped cell bodies, sends axonal terminals (triangles) back into the MB lobes as part of a feedforward network. (See (26) for more details.) The α1 compartment is the one MB compartment whose activity consistently influenced feeding behavior (both PER and consumption). This diagram was modified from Fig. 17 in (26).

Chapter 3

Developing a strategy for monitoring neural activity during learning

SUMMARY

While the experiments in Chapter 2 describe MB neurons that influence proboscis extension, they left open the broader question of how neural activity changes on a larger scale during learning. MB outputs integrate sensory information and valence, transmitting signals downstream to ultimately talk to sugar-responsive neurons including motor neurons of the taste-processing center, the sub-esophageal zone (SEZ). To study the brain in the context of learning, we chose an aversive taste-conditioning paradigm, and sought to track neuronal changes in the SEZ during learning, using calcium imaging. During this set of experiments, we explored and improved methods for large-scale calcium imaging. We tested a variety of unconditioned stimuli (US) and experimental conditions to determine the optimal conditions for robust taste learning. We also developed a pipeline for analyzing whole-subesophageal zone (SEZ) calcium imaging data.

INTRODUCTION

The idea that memory formation is rooted in changes in the strength of neural connections dates as far back as Cajal (112), more than a century ago. The idea that synaptic strength changes during learning and memory was refined into an elegant concrete model by Hebb in 1949 (113), in which learning and memory occur through synaptic modification as a result of coincident pre- and postsynaptic activity. Experimental evidence of synaptic plasticity in the mammalian brain came about 20 years later with the discovery of long-term potentiation (LTP) (114). In a set of groundbreaking experiments, high-frequency stimulation (called a tetanus) of hippocampal excitatory synapses produced a rapid and long-lasting increase in the strength of the synapses that persisted for many days (115). LTP, which has been described at synapses throughout the brain, remains one of the most attractive cellular models for learning and memory (116, 117). How though, do cellular changes translate into measurable behavioral changes? Electrical recordings from one or two neurons at a time deep in the brain provides insight into synaptic changes and the conditions that strengthen or weaken individual connections. Yet, neurons function in highly interconnected and distributed networks that are modulated over a wide range of time scales. To observe how networks encode, store, and retrieve information, we need experimental methods aligned with manipulating, and tracking changes in, large ensembles of neurons in behaving animals.

Functional optical imaging

One method to manipulate and record from many neurons simultaneously is functional optical imaging. This approach uses microscopic methods to deliver excitation light and collect emitted photons, to allow observation of regions of interest. Within the last decade, a wealth of genetic tools for optical imaging have been developed and refined to allow direct observation and highly specific manipulation of neurons in the *Drosophila* central nervous system.

For example, genetically encoded calcium indicators feature significantly higher signal-to-noise than they did 1.5 decades ago. These indicators work by increasing fluorescence in response to increases in intracellular Ca^{2+} ion concentration. Nearly all neuron types express voltage-sensitive Ca^{2+} channels (118), which flux calcium ions into the cell upon neural membrane depolarization (119–121). Since calcium enters a neuron whenever it fires, detecting changes in calcium levels is a good proxy for recording neuronal activity. The archetypal calcium indicator is GCaMP, a chimeric protein in which a circularly permuted (*i.e.*, given new N- and C-termini) Green Fluorescent Protein (GFP) is fused to the calcium-binding protein calmodulin. Roughly speaking, the calmodulin acts as a sensor, and GFP is a shape-shifter, changing shape in the presence of calcium. This structural rearrangement increases fluorescent output. This activity can be detected with a microscope, allowing the researcher to directly visualize of neural activity.

The last decade has also seen advances in genetic tools that allow spatially precise access to neurons. “Optogenetics” refers to the use of light to manipulate the activity of specific neurons, to activate or silence them in a temporally controlled manner. The vast collection of tools available for targeting defined cell populations in flies (*e.g.*, the binary expression systems such as Gal4, split-Gal4, LexA, and Q) allows experiments in flies

that are not possible in other animal models. The fruit fly *Drosophila Melanogaster* is thus an excellent model to probe questions about neuronal changes that occur in the brain during learning. Just as its genes have made informative contributions to our understanding of development, function, and diseases of the human nervous system, the architecture and computations of *Drosophila* neural circuits may also provide insightful clues into mammalian brain function.

Learning in *Drosophila*

The most widely studied learning in *Drosophila* is olfactory conditioning. In this type of learning, flies learn to associate a neutral odor (conditioned stimulus, CS) with a positive or negative stimulus (unconditioned stimulus, US) through paired presentation. Memory retention and retrieval is usually assayed by recording the population preference of flies forced to choose between the trained odor and an untrained odor.

Another type of associative learning observed in flies is taste conditioning. In this conditioning paradigm, flies can be trained to reject sweet tastants when they are paired with an aversive stimulus such as a noxious pulse of an infrared laser (8), or a bitter tastant (9, 11). The taste conditioning circuit begins in the peripheral nervous system, where gustatory perception in the fly is initiated by the binding of tastants to receptors expressed on gustatory neurons of the proboscis, mouthparts, legs, and wings (21). These receptors detect different taste modalities including sugar, bitter, and water (122) and upon tastant binding cause activation of gustatory neurons. Gustatory neurons send projections to the SEZ in *Drosophila* (21), and subsequently information is relayed to higher brain regions including the MB, before being relayed back to the SEZ, where motor neurons driving PER behavior are located (93). While some pathways from the SEZ to higher brain regions have been identified (123), they are not well characterized. There is a larger gap in knowledge about the flow of information out of the MB, and how it impinges on behavioral output.

Taste conditioning in *Drosophila* is an attractive system to address how neural circuits encode memory and guide behavioral changes for two reasons: the availability of a clear behavioral readout (proboscis extension, PER) and a priori knowledge of the final step of the relay (the location of the motor neurons driving PER.)

One approach to understanding decision-making processes is to identify sites of synaptic plasticity underlying memory formation, and examine the postsynaptic neurons that transmit stored information to the downstream circuit in order to discover how their altered activities bias behavior. Because there is a clear behavioral readout of learning (proboscis extension), learning can potentially be tracked in a single fly. In this study, we developed a large-scale calcium imaging method to capture neural responses in the SEZ, the taste-processing center, in single flies before, during, and after taste conditioning. As pairing detection of sucrose by leg gustatory neurons with bitter detection by proboscis gustatory neurons inhibits proboscis extension to sucrose, we hypothesized that there would be fewer sugar-responsive neurons in the SEZ after taste conditioning, because PER-causing motor neurons should not be activated. Previous studies have used calcium imaging to determine how neural activity correlates with sensory input or behavior output. Those studies revealed specific neurons in the subesophageal zone (SEZ) which are activated by sensory detection of different taste modalities (111, 124). In this study,

we combined previously established calcium imaging methods with new tools and a learning paradigm.

RESULTS

Developing a method to monitor learning under the scope

We used a spinning disc confocal microscope to record calcium responses to leg presentations of sucrose in a live fly before, during, and after learning (Fig. 3.1). Specifically, we expressed the genetically encoded calcium indicator nls-GCaMP6s (chosen for its high sensitivity, low basal fluorescence, and slow decay) using the pan-neural promoter *nSynaptobrevin-Gal4*. Nuclear GCaMP6 (Dickson lab, unpublished) allows visualization of discrete cells, facilitating analysis without the addition of an additional transgene to mark individual cells, as was necessary in previous studies with cytosolic GCaMP. To cover the entire SEZ, we continuously scanned 20 z-sections with 1.2 μm spacing, 100 ms exposure.

In our setup (Fig. 3.1A), we used 2 IR cameras to visualize the sugar stimulus, and to record proboscis movements. A high-resolution IR camera allowed visualization of the proboscis from the side, in conjunction with a customized imaging chamber (with short arms to give an unobstructed view of the proboscis.) During the dissection for the *in vivo* prep, we tried to only wax half of the proboscis so that we could visualize proboscis extension.

For the learning paradigm, we used conditioned taste aversion to train flies (Fig. 3.1B). This involves (1) the pretest: a sucrose presentation to the legs, followed by (2) training: 3 pairings of sucrose to the legs with thermogenetic bitter to the proboscis, followed by (3) the testing phase: sucrose presentation to the legs. The thermogenetic bitter stimulus was chosen in place of a physical bitter presentation because of limited space under the microscope, and was achieved by using the *Gr66a-Gal4* promoter to drive the expression of a heat-sensitive cation channel dTrpA1 in bitter sensing neurons. A previous study showed that stimulating the proboscis with heat via an IR laser in *Gr66a > dTrpA1* flies is sufficient for conditioned taste aversion (36).

Pipeline for data analysis

We created a pipeline for data analysis (Fig. 3.2A). The data from all z-sections was compressed into a single 2-dimensional image for each time point by applying a maximum to each x-y coordinate (MaxZ). Most taste-responsive cells are contained within the top layers of the SEZ (111), so we chose an imaging volume that would encompass these. Importantly, the taste-responsive cells are non-overlapping (111), so the MaxZ projection gives an accurate proxy of responding cells. In addition to requiring less processing power for data analysis, the MaxZ projection is also attractive because it provides a solution to z-motion correction, since the responding cells would be contained within each z-stack.

In the pipeline, we used FIJI to analyze images. First, xy motion was corrected using ImageStabilizer. After motion correction, we manually drew regions of interest (ROIs) around the circular nuclei and saved the positions. The fluorescence intensities within those ROIs were measured and exported for further analysis using R. In R, we

performed baseline subtraction and calculated the change in fluorescence divided by baseline fluorescence (ΔF/F) for each ROI. We were interested in seeing which cells that responded in the pretest also responded after learning, so we thresholded 'active' cells. Finally, for visualization purposes, the locations of responding cells were projected onto single image for each stimulation (Pre-test, Trial 1, Trial 2, Trial 3, Testing). These representative heat-maps provide a qualitative evaluation of whether sucrose-responsive cells at each stimulation are stereotyped between brains. (Fig. 3.2B). In addition to the spatial heat maps, fluorescent traces of individual responding cells were also plotted (Fig. 3.2B).

The search for a robust learning phenotype

While flies are able to learn under the conditioned taste paradigm with Gr66a as the US, we found that the learning was not robust, with only 30% of starved flies showing proboscis extension suppression during the testing phase (Fig.3.3A). We tried varying the age of flies under different starvation conditions, and found that older flies showed the most robust learning phenotype, with no difference between starved and fed flies. The presence of many transgenes (*nsyb-Gal4*, *UAS-nlsGCaMP6s*, *UAS-Histone-mRFP, Gr66a-LexA,* and *LexAop-dTrpA1*) may explain why these flies did not perform as well in the learning paradigm as flies expressing fewer transgenes (i.e. only *Gr66a-LexA* and *LexAop-dTrpA1*), which showed PER suppression in 70% of flies (Fig 3.3B).

Dissecting the fly for imaging only made the learning less robust (data not shown.) This observation led us to try re-sealing the dissected brain, to create an imaging window in an otherwise intact fly. Here, dissected flies sealed with ultraviolet (UV) glue, flies were healthy enough to survive overnight and walk around after being released from the imaging chamber. The UV glue, however, caused distortion of the imaging plane, making analysis difficult.

Due to the poor learning encountered in dissected animals using Gr66a as a US, we explored other potential candidates for the US (Fig. 3.3C). We crossed a variety of *Gr*-Gal4's to *UAS-CsChrimson*, and paired a red laser with sucrose leg presentation during the taste-conditioning paradigm. Among the Gal4 lines tested, we found that Gr89a was the best US in fed flies, resulting in the strongest aversion post-learning, comparable to similar to Gr66a in fed flies. Under fed conditions, approximate 90% of flies punished by Gr89a neural activation did not extend their proboscis, suggesting reliable learning in single flies. For comparison, approximately 80% of flies punished by Gr66a activation did not extend their proboscis during the testing phase. Since Gr89a is only available as a Gal4 and not LexA line, and the *nsyb-LexA* drivers did not produce viable progeny with nls-GCaMP, we concluded that Gr66a was still the best US.

In our quest for flies that exhibit robust learning, we also considered training a large number of flies, selecting the flies that exhibited the most robust learning, and then imaging whole-SEZ sucrose responses in those selected flies. With this approach, we would compare sucrose responses in trained flies vs. untrained flies only at a population level. To achieve high-throughput conditioning, flies were trained in the STROBE system, which allows training of 16 flies simultaneously (125). Briefly, flies expressing CsChrimson under the control of the Gr66a promoter were placed inside closed-loop optogenetic stimulation chambers. Feeding behavior is quantified using capacitive proximity sensors on 2 different food sources (25mM sucrose in agar or 1% agar). A

single fly is placed in each chamber, free to choose between those 2 food sources throughout a training phase and a testing phase. During training, red lights flash whenever a fly makes contact with the 25mM sucrose in agar, thereby activating the bitter-sensing Gr66a fibers in a closed-loop aversive conditioning paradigm. After training, flies are given a choice between plain agar and the 25mM sucrose in agar, and the number of interactions with each substance is recorded. Using the STROBE system for aversive taste conditioning, trained flies showed a reduced preference for the sugar (Fig. 3.4). In these experiments, the strength of the learning phenotype was highly variable – while animals do learn, there are still many animals that do not learn, as seen by the estimated probability densities (Fig 3.4). The STROBE system allows for training large numbers of animals, and would allow us to select the flies that exhibit the strongest learning phenotype. Whether the memory is robust enough to survive the dissection for imaging under the scope remains to be determined. Also, comparing responses across different fly brains poses a challenge and remains as future work.

DISCUSSION

Most behavioral and learning assays in *Drosophila* have been reported as population studies. How well a single animal learns has a probabilistic component – some animals behave in a predictable way, while others do not act as predicted. In this study, we set out to study learning by monitoring neural activity in single animals, specifically we aimed to understand how the sugar-responsive network of neurons in the SEZ is influenced by a taste-conditioning paradigm.

Our efforts resulted in a number of methodological advances: first, we explored and developed an improved preparation for imaging, allowing for better visibility of sensory stimulus delivery to flies during calcium imaging, as well as high resolution visualization of the proboscis to track possible extensions throughout the learning process. We also developed a pipeline for data analysis of calcium responses to sucrose in the SEZ. Additionally, we found favorable conditions that allow single flies to learn, and determined that activation of Gr66a is the most reliable CS for aversive taste conditioning.

The obstacles we encountered in imaging SEZ neurons during taste learning largely relate to the difficulty of measuring whether individual flies properly learned. During the taste conditioning paradigm in flies glued to a slide, the distinction between flies that learned and flies that didn't is clear: a fly that learned will no longer extend its proboscis, whereas a fly that didn't learn will still extend. We tried to visualize the proboscis during the calcium imaging experiment by using a high-resolution camera to record proboscis movements. In order to visualize the SEZ, though, the proboscis must be moved and waxed out in order to not obscure the neurons of interest. We also tried to record calcium changes in various motorneurons required for the proboscis extension motor program, as a metric for successful learning. Most of those neurons are obscured in our *in vivo* prep, and because the proboscis is waxed out to allow an unencumbered view of the SEZ, it appeared that the motor neurons were firing independent of proboscis movement in the video visualization. Without a clear readout for learning, it was impossible for us to determine which flies had successfully undergone learning. Since the rate of learning had high variability between flies (Fig. 3.3, 3.4), having a behavioral

readout was especially important – it is possible that some flies we tried imaging were not in the population of 'robust learners.' Therefore, we were not able to compare between an untrained and trained state. Perhaps a different setup for imaging a fly in a 'happier' state such as a fly on a ball might allow for more robust and natural behavior. Despite the setbacks, we believe that the methods we developed, and this documentation of our attempts at imaging during learning should be a useful reference for others who subsequently work on this problem.

Figure 3.1

A

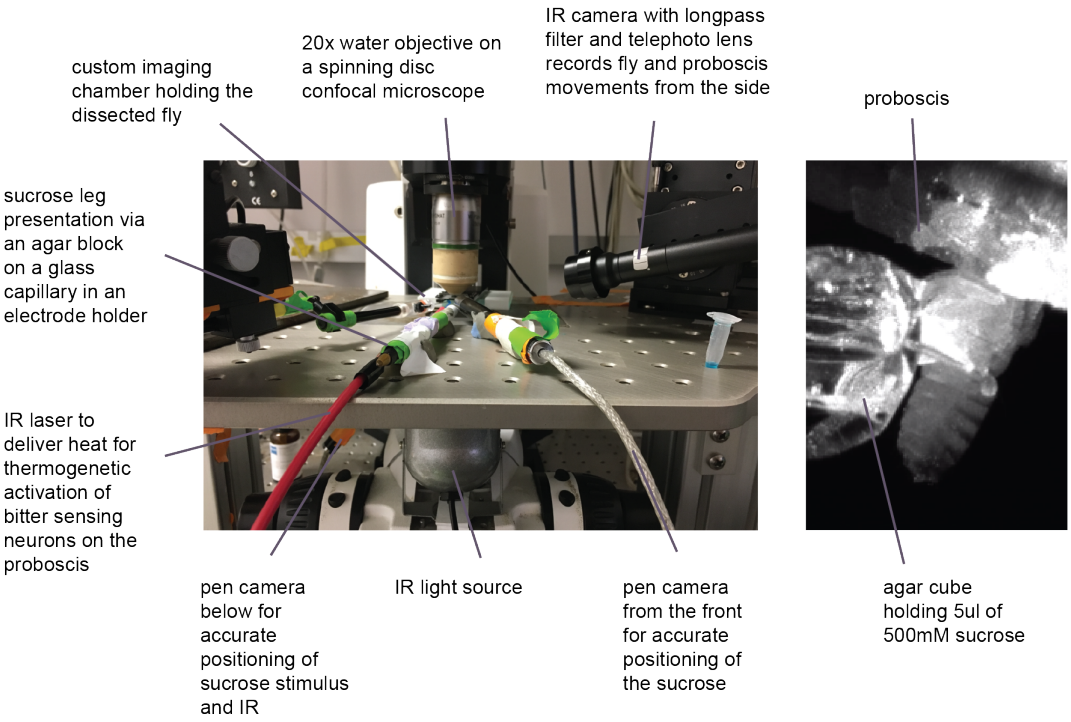

B

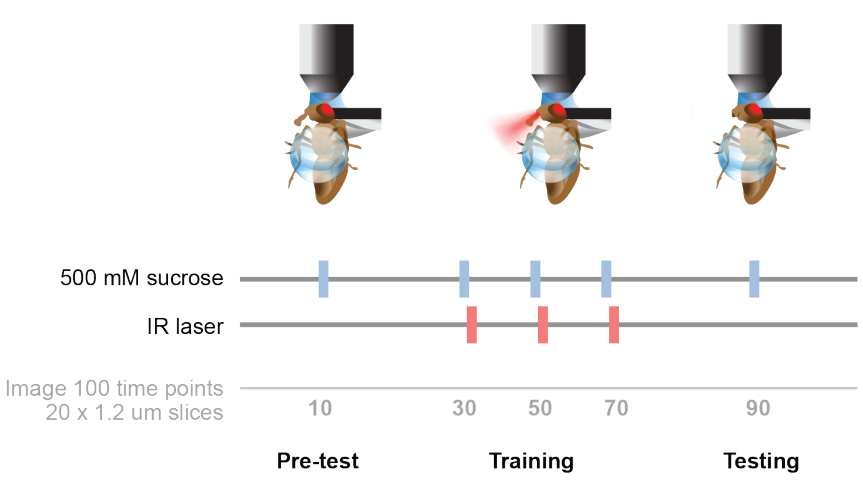

Figure 3.1. Imaging setup and stimulation protocol. A) Imaging setup. Left: Photo with callouts describing the experimental setup. Right: Representative still image from the high-resolution IR camera showing the proboscis. B) Schematic showing the learning paradigm: 20 z-sections with 1.2µm spacing captures the entire SEZ. 100 times points total are imaged. At time point 10, 500 mM sucrose is delivered to the tarsi for 2 time points. During training, at time points 30, 50, and 70, 500 mM sucrose is manually delivered to the tarsi, paired with a 2s pulse of IR light controlled with a foot pedal. Finally, at time point 90, sucrose is delivered to the tarsi.

Figure 3.2

A

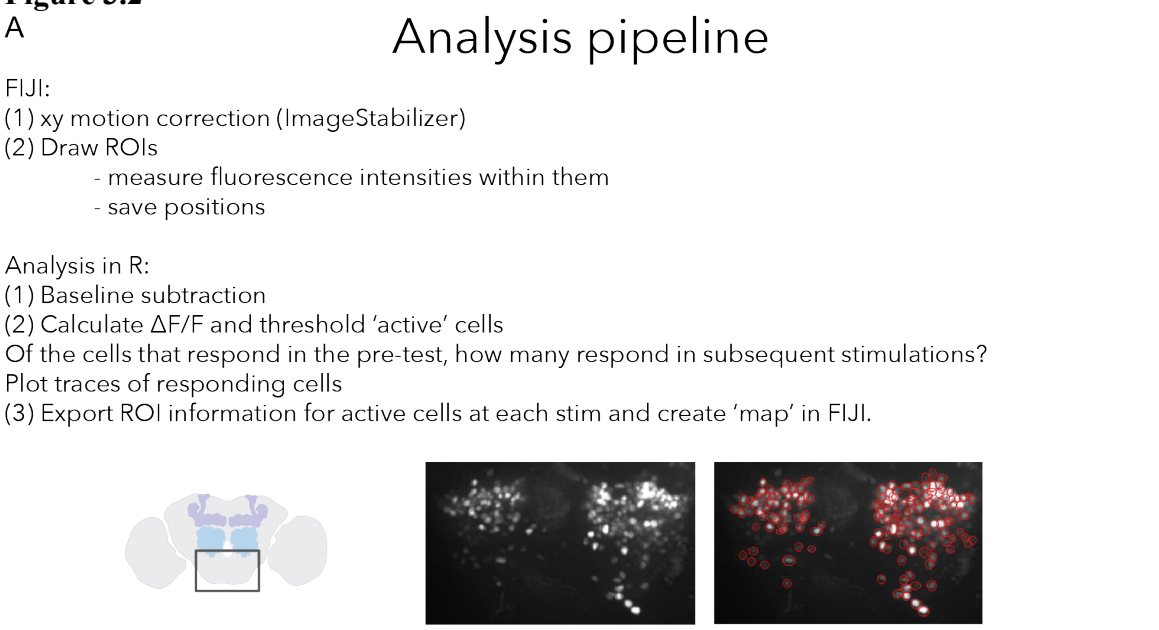

B

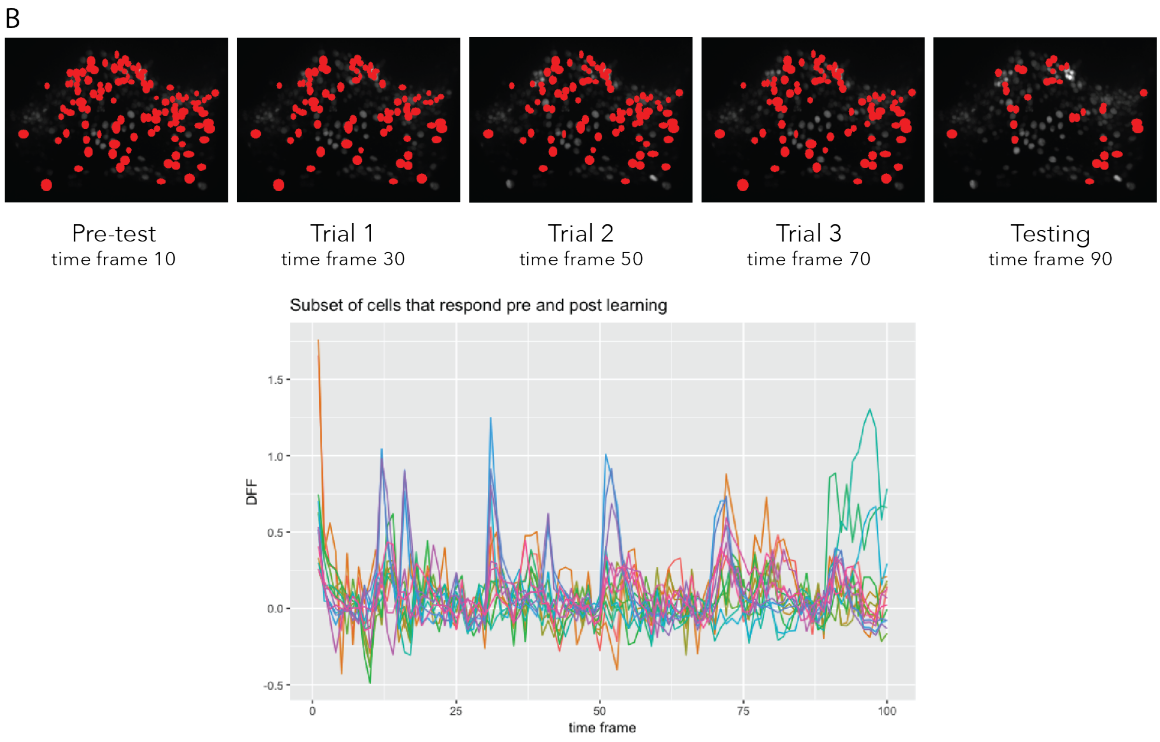

Figure 3.2. Analysis of calcium imaging data from learning experiments.
A) Overview of the pipeline for data analysis using FIJI and R. B) Representative data showing analysis from one fly. Top: Red circles are sucrose-responsive cells at each testing time point indicated (pre-test, trial 1, trial 2, trial 3, and test). Bottom: ΔF/F traces for sucrose-responsive cells, each line is one neuron.

Figure 3.3

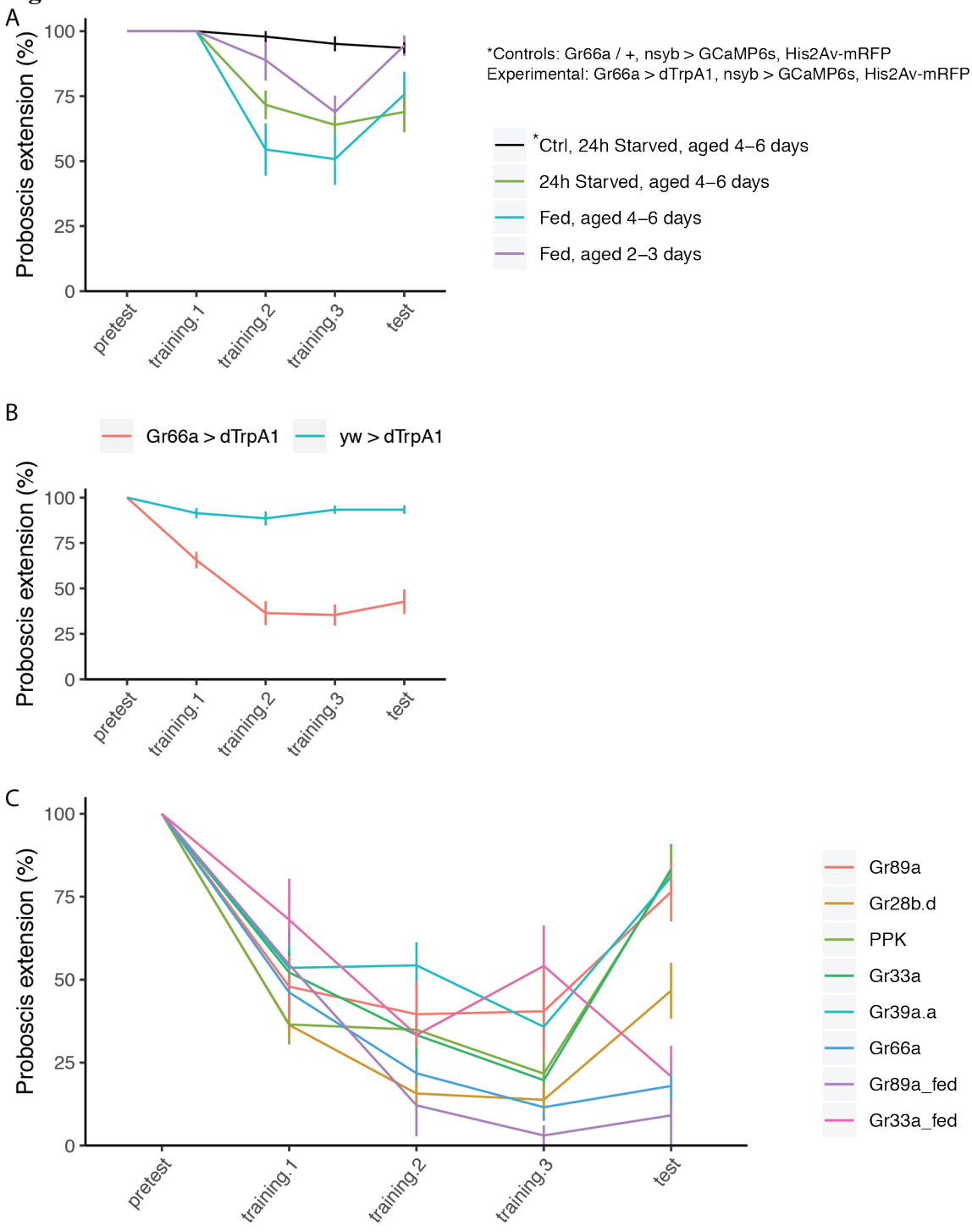

Figure 3.3 Searching for another candidate US.
A) Optimizing for hunger state and age in the learning assay: *Gr66a > dTrpA1, nsyb > nls-GCaMP6s* flies were tested for aversive taste memory under 24h starved or satiated, in younger (2-3 days old) and older (4-6 days old) mated female flies. Proboscis

extension to 500mM sucrose was tested during the pretest (sucrose on the tarsi), 3 training trials (paired sucrose on the tarsi with IR laser for thermogenetic activation of *Gr66a > dTrpA1* neurons), and a test trial (500 mM sucrose to the tarsi.) Error bars represent the SEM (n = 14-44 flies per condition / genotype). B) Aversive taste conditioning for PER in Gr66a, dTrpA1 flies results in robust learning when 500mM sucrose is paired with IR heat activation in experimental, but not control flies. C) A variety of Gr-Gal4 lines were selected and tested as a possible US. Error bars represent the SEM, n = 11 – 34 flies per genotype / condition.

Figure 3.4

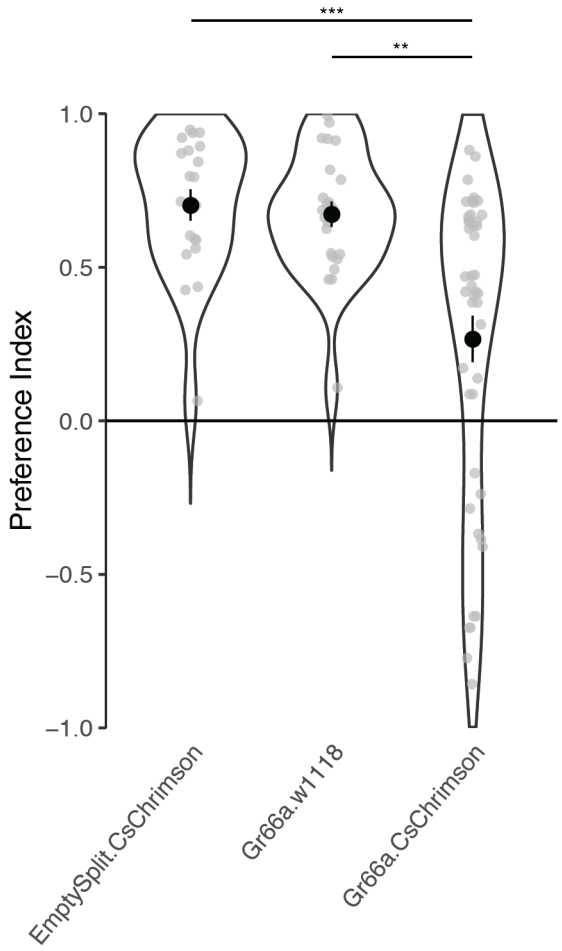

Figure 3.4 Flies learn to prefer sugar less in an aversive taste-conditioning paradigm in the STROBE.
Female flies (3-7 days old) were placed on retinal food or standard food (controls) for 2 days, followed by 24 hr starvation on retinal / non-retinal agar. During the 40-minute training in the STROBE, flies were free to choose between (1) 25 mM sucrose paired with red light to activate bitter-sensing Gr66a neurons whenever the fly interacted with the sucrose, or (2) 1% agar (no red light). Training was followed by a 10-minute rest period in individual starvation vials. Finally, during the 60-minute testing phase, LEDs were deactivated. Preference Index = (Interactions with 25mM sucrose – Interactions with agar) / (total interactions) for the 40 minute (training) or 1 hr (testing) timeframe. Grey dots represent individual flies, black dot and whiskers represent mean +- SEM. Statistical significance was determined with Wilcoxon Rank test with Bonferroni correction for multiple comparisons, **$p < 0.01$, *** $p < 0.001$, $n = 20$-46. This data was reproduced with the permission of Meghan Jelen and Mike Gordon (unpublished).

Chapter 4:

Discussion

An ability to modulate behavior based on prior experiences is key to survival. Distinguishing between 'good' and 'bad' guides our choices as we navigate the world. Our sensory systems provide information to allow us to perform a qualitative analysis of our surroundings, and our memory centers allow us to learn and update our preferences in ever-changing surroundings. For example, the sweet taste of sugar is innately appetitive to both flies and humans – even from an early age, most of us reach for ice cream and lollipops over brussel sprouts and broccoli. Yet, we learn to modulate our preferences over time – too much sugar may cause a headache, or have negative implications for your aspirational beach bod. Learning many also happen rapidly - perhaps a single food poisoning event turns you off of a previously delicious food forever. In either case, our internal systems of reward and punishment assign appropriate values to our actions and interactions. We evaluate the valence and magnitude of stimuli, and these signals become integrated in the brain to guide behavior. Can our entire existence, then, be reduced to a simplistic model of approach or avoidance? Probably (I hope) not. Experiences and behaviors are complex and intricate. With the ultimate goal of understanding the complexity of human behavior, we turn to simpler model organisms. The hope is that by understanding more completely a simpler system and model, we can extrapolate and apply our findings more broadly in the future.

In the studies presented in this thesis, we examined the modulation of a simple behavioral response (proboscis extension) to food in the fruit fly. In Chapter 2, we show that neural activity in the specific outputs of the mushroom body (MB), the learning and memory center of the fly brain, is able to modify and strongly suppress the innate response to sugar. Silencing those neurons, however, does not have a strong reciprocal effect. We also looked at the effect of activating the dopaminergic inputs into the mushroom body, and found a few that also suppress proboscis extension. Finally, we determined that broader feeding behavior is influenced by mushroom body output neuron activity, as shown by sugar consumption time. Interestingly, the set of output neurons whose activation suppresses proboscis extension doesn't entirely overlap with the set of neurons previously determined to drive approach or avoidance behavior (26). Additionally, we find that the MB outputs whose activation suppresses proboscis extension are not responsive to sucrose. Finally, we describe putative downstream neurons to begin connecting the dots between the mushroom body and motor outputs. In Chapter 3, we extend the behavioral studies described in chapter 2 to gain a better understanding of the neural circuit that functionally influences feeding behavior. We describe a large-scale calcium imaging approach to track the sugar-responsive network of neurons in the SEZ (subesophageal zone, the taste-processing center of fruit flies) during an aversive taste-conditioning paradigm.

This work contributes to the larger field of invertebrate behavioral modulation. Even innate behaviors like responses to taste responses to sugar can be modified through learned associations, and here we find evidence for a distributed mushroom body network. Taste and feeding behaviors are modulated by MB activity and funneled through outputs that are not necessarily the same outputs of the MB that drive avoidance and approach. Yet, it is not a single compartment that drives changes in feeding behavior.

Outlook and future directions

The methodology described in Chapter 3 for imaging a live animal during learning lays the groundwork for future studies. A different type of preparation such as a fly walking on a ball may be suitable for imaging during learning, in order to provide the best possible conditions for robust taste learning to occur. We tried activating several subsets of bitter-and-pain sensing neurons as the unconditioned stimulus (US) and found that Gr66a provided the strongest learning phenotype. Taste learning still seems like a great system to study learning because of the clear behavioral output (proboscis extension.) Future experiments might test whether pairing taste with a stronger unconditioned stimulus (US) like a shock yields more robust learning.

The pathways from the MB to the motor neurons for proboscis extension it the SEZ are still unknown. The results from our trans-Tango experiments give a glimpse of the areas of the brain that mostly likely receive synaptic inputs. By comparing these heat maps with the expression patterns of Gal4 drivers in existing databases, we may identify candidate downstream neurons, and then validate connections using functional connectivity (optogenetic activation of the pre-synaptic neuron while recording from the post-synaptic candidate neuron.)

In addition to the downstream pathways relaying information from the MB to the SEZ motor neurons, the upstream pathways from the SEZ to the MB are also not entirely understood. Some pathways conveying taste information from the SEZ to the higher brain have been described, but questions remain about how many of these pathways exist and why. There is evidence that the state of an animal influences reward pathways (for example, a hungry animal values food more than a satiated one). Some hunger modulation occurs at the sensory level: calcium responses of sugar sensory neurons are greater in starved flies than in fed flies (111). Hunger modulation likely occurs at central sites as well, as sugar activates PAM-DANs (32), and the magnitude of the calcium responses differs greatly between starved and fed animals.

Although we are far from understanding the function of the mushroom body in its entirety, the wealth of tools available positions us well in the search for answers. *Drosophila* studies, like the ones described in this dissertation, make use of binary expression systems (e.g. UAS/Gal4) to drive expression of transgenes in subpopulations of neurons. Intersectional methods like the Split-Gal4 system allow for further restriction to highly specific targeted expression. In recent years, large-scale efforts to develop cell-type specific tools have yielded unprecedented genetic access to small populations of neurons. The continuing advancement of these tools will allow the *Drosophila* community to investigate behaviors and pinpoint causal neurons for behavior with greater precision than ever before. The signal to noise of calcium and voltage indicators are becoming increasingly better, in conjunction with the development of better optics and faster acquisition rates; together, these tools will allow us to observe neural circuits with single-cell resolution in real time. Simultaneously, EM tracing is revealing synaptic connections and previously unknown circuit motifs. This is an exciting time for the field of neuroscience, with a wealth of capabilities on the horizon to address circuit-level questions about behavioral modulation.

References

1. Garcia J, Kimeldorf DJ, Koelling RA (1955) Conditioned aversion to saccharin resulting from exposure to gamma radiation. *Science* 122(3160):157–158.

2. Reilly S, Schachtman TR (2009) *Conditioned Taste Aversion: Neural and Behavioral Processes* (Oxford University Press).

3. Garcia J, Ervin FR, Koelling RA (1966) Learning with prolonged delay of reinforcement. *Psychonomic Science* 5(3):121–122.

4. Davis RL (1993) Mushroom bodies and Drosophila learning. *Neuron* 11(1):1–14.

5. Griffith LC, Ejima A (2009) Courtship learning in Drosophila melanogaster: diverse plasticity of a reproductive behavior. *Learn Mem* 16(12):743–750.

6. Kahsai L, Zars T (2011) Learning and memory in Drosophila: behavior, genetics, and neural systems. *Int Rev Neurobiol* 99:139–167.

7. Menda G, et al. (2011) Classical conditioning through auditory stimuli in Drosophila: methods and models. *J Exp Biol* 214(Pt 17):2864–2870.

8. Masek P, Scott K (2010) Limited taste discrimination in Drosophila. *Proc Natl Acad Sci U S A* 107(33):14833–14838.

9. Kirkhart C, Scott K (2015) Gustatory learning and processing in the Drosophila mushroom bodies. *J Neurosci* 35(15):5950–5958.

10. Masek P, Keene AC (2016) Gustatory processing and taste memory in Drosophila. *J Neurogenet* 30(2):112–121.

11. Masek P, Worden K, Aso Y, Rubin GM, Keene AC (2015) A dopamine-modulated neural circuit regulating aversive taste memory in Drosophila. *Curr Biol* 25(11):1535–1541.

12. Quinn WG, Harris WA, Benzer S (1974) Conditioned behavior in Drosophila melanogaster. *Proc Natl Acad Sci U S A* 71(3):708–712.

13. Tempel BL, Bonini N, Dawson DR, Quinn WG (1983) Reward learning in normal and mutant Drosophila. *Proc Natl Acad Sci U S A* 80(5):1482–1486.

14. Galili DS, et al. (2014) Converging circuits mediate temperature and shock aversive olfactory conditioning in Drosophila. *Curr Biol* 24(15):1712–1722.

15. Das G, et al. (2014) Drosophila learn opposing components of a compound food stimulus. *Curr Biol* 24(15):1723–1730.

16. Burke CJ, Waddell S (2011) Remembering nutrient quality of sugar in Drosophila. *Curr Biol* 21(9):746–750.

17. Lin S, et al. (2014) Neural correlates of water reward in thirsty Drosophila. *Nat Neurosci* 17(11):1536–1542.

18. Heisenberg M (2003) Mushroom body memoir: from maps to models. *Nat Rev Neurosci* 4(4):266–275.

19. McGuire SE, Deshazer M, Davis RL (2005) Thirty years of olfactory learning and memory research in Drosophila melanogaster. *Prog Neurobiol* 76(5):328–347.

20. Laissue PP, et al. (1999) Three‐dimensional reconstruction of the antennal lobe in Drosophila melanogaster. *The Journal of Comparative Neurology* 405(4):543–552.

21. Stocker RF (1994) The organization of the chemosensory system in Drosophila melanogaster: a review. *Cell Tissue Res* 275(1):3–26.

22. Liang, et al. (2013) GABAergic Projection Neurons Route Selective Olfactory Inputs to Specific Higher-Order Neurons. *Neuron* 79(5):917–931.

23. Ito K, et al. (1998) The organization of extrinsic neurons and their implications in the functional roles of the mushroom bodies in Drosophila melanogaster Meigen. *Learn Mem* 5(1-2):52–77.

24. Lin H-H, Chu L-A, Fu T-F, Dickson BJ, Chiang A-S (2013) Parallel neural pathways mediate CO2 avoidance responses in Drosophila. *Science* 340(6138):1338–1341.

25. Aso Y, et al. (2009) The mushroom body of adult Drosophila characterized by GAL4 drivers. *J Neurogenet* 23(1-2):156–172.

26. Aso Y, et al. (2014) The neuronal architecture of the mushroom body provides a logic for associative learning. *eLife* 3. doi:10.7554/elife.04577.

27. Lee T, Lee A, Luo L (1999) Development of the Drosophila mushroom bodies: sequential generation of three distinct types of neurons from a neuroblast. *Development* 126(18):4065–4076.

28. Crittenden JR, Skoulakis EM, Han KA, Kalderon D, Davis RL (1998) Tripartite mushroom body architecture revealed by antigenic markers. *Learn Mem* 5(1-2):38–51.

29. Schroll C, et al. (2006) Light-induced activation of distinct modulatory neurons triggers appetitive or aversive learning in Drosophila larvae. *Curr Biol* 16(17):1741–1747.

30. Claridge-Chang A, et al. (2009) Writing memories with light-addressable reinforcement circuitry. *Cell* 139(2):405–415.

31. Aso Y, et al. (2010) Specific dopaminergic neurons for the formation of labile aversive memory. *Curr Biol* 20(16):1445–1451.

32. Liu C, et al. (2012) A subset of dopamine neurons signals reward for odour memory in Drosophila. *Nature* 488(7412):512–516.

33. Aso Y, et al. (2014) Mushroom body output neurons encode valence and guide memory-based action selection in Drosophila. *Elife* 3:e04580.

34. Owald D, et al. (2015) Activity of defined mushroom body output neurons underlies learned olfactory behavior in Drosophila. *Neuron* 86(2):417–427.

35. Hige T, Aso Y, Modi MN, Rubin GM, Turner GC (2015) Heterosynaptic Plasticity Underlies Aversive Olfactory Learning in Drosophila. *Neuron* 88(5):985–998.

36. Keene AC, Masek P (2012) Optogenetic induction of aversive taste memory. *Neuroscience* 222:173–180.

37. Yapici N, Cohn R, Schusterreiter C, Ruta V, Vosshall LB (2016) A Taste Circuit that Regulates Ingestion by Integrating Food and Hunger Signals. *Cell* 165(3):715–729.

38. Falk R, Bleiser-Avivi N, Atidia J (1976) Labellar taste organs of Drosophila melanogaster. *J Morphol* 150(2):327–341.

39. Fujishiro N, Kijima H, Morita H (1984) Impulse frequency and action potential amplitude in labellar chemosensory neurones of Drosophila melanogaster. *Journal of Insect Physiology* 30(4):317–325.

40. Hiroi M, Marion-Poll F, Tanimura T (2002) Differentiated response to sugars among labellar chemosensilla in Drosophila. *Zoolog Sci* 19(9):1009–1018.

41. Meunier N, Marion-Poll F, Rospars J-P, Tanimura T (2003) Peripheral coding of bitter taste in Drosophila. *J Neurobiol* 56(2):139–152.

42. Dahanukar A, Lei Y-T, Kwon JY, Carlson JR (2007) Two Gr genes underlie sugar reception in Drosophila. *Neuron* 56(3):503–516.

43. Jiao Y, Moon SJ, Montell C (2007) A Drosophila gustatory receptor required for the responses to sucrose, glucose, and maltose identified by mRNA tagging. *Proc Natl Acad Sci U S A* 104(35):14110–14115.

44. Dunipace L, Meister S, McNealy C, Amrein H (2001) Spatially restricted expression of candidate taste receptors in the Drosophila gustatory system. *Curr Biol* 11(11):822–835.

45. Scott K, et al. (2001) A chemosensory gene family encoding candidate gustatory and olfactory receptors in Drosophila. *Cell* 104(5):661–673.

46. Thorne N, Chromey C, Bray S, Amrein H (2004) Taste Perception and Coding in Drosophila. *Current Biology* 14(12):1065–1079.

47. Wang Z, Singhvi A, Kong P, Scott K (2004) Taste representations in the Drosophila brain. *Cell* 117(7):981–991.

48. Weiss LA, Dahanukar A, Kwon JY, Banerjee D, Carlson JR (2011) The molecular and cellular basis of bitter taste in Drosophila. *Neuron* 69(2):258–272.

49. Fischler W, Kong P, Marella S, Scott K (2007) The detection of carbonation by the Drosophila gustatory system. *Nature* 448(7157):1054–1057.

50. Zhang YV, Ni J, Montell C (2013) The molecular basis for attractive salt-taste coding in Drosophila. *Science* 340(6138):1334–1338.

51. Koh T-W, et al. (2014) The Drosophila IR20a clade of ionotropic receptors are candidate taste and pheromone receptors. *Neuron* 83(4):850–865.

52. Ganguly A, et al. (2017) A Molecular and Cellular Context-Dependent Role for Ir76b in Detection of Amino Acid Taste. *Cell Rep* 18(3):737–750.

53. Chen Y, Amrein H (2017) Ionotropic Receptors Mediate Drosophila Oviposition Preference through Sour Gustatory Receptor Neurons. *Curr Biol* 27(18):2741–2750.e4.

54. Adams CM, et al. (1998) Ripped pocket and pickpocket, novel Drosophila DEG/ENaC subunits expressed in early development and in mechanosensory neurons. *J Cell Biol* 140(1):143–152.

55. Zelle KM, Lu B, Pyfrom SC, Ben-Shahar Y (2013) The Genetic Architecture of Degenerin/Epithelial Sodium Channels inDrosophila. *G3: Genes|Genomes|Genetics* 3(3):441–450.

56. Cameron P, Hiroi M, Ngai J, Scott K (2010) The molecular basis for water taste in Drosophila. *Nature* 465(7294):91–95.

57. Chen Z, Wang Q, Wang Z (2010) The amiloride-sensitive epithelial Na+ channel PPK28 is essential for drosophila gustatory water reception. *J Neurosci* 30(18):6247–6252.

58. Liu T, Starostina E, Vijayan V, Pikielny CW (2012) Two Drosophila DEG/ENaC channel subunits have distinct functions in gustatory neurons that activate male courtship. *J Neurosci* 32(34):11879–11889.

59. Lu B, LaMora A, Sun Y, Welsh MJ, Ben-Shahar Y (2012) ppk23-Dependent chemosensory functions contribute to courtship behavior in Drosophila melanogaster. *PLoS Genet* 8(3):e1002587.

60. Thistle R, Cameron P, Ghorayshi A, Dennison L, Scott K (2012) Contact chemoreceptors mediate male-male repulsion and male-female attraction during Drosophila courtship. *Cell* 149(5):1140–1151.

61. Toda H, Zhao X, Dickson BJ (2012) The Drosophila female aphrodisiac pheromone activates ppk23(+) sensory neurons to elicit male courtship behavior. *Cell Rep* 1(6):599–607.

62. Vosshall LB, Stocker RF (2007) Molecular architecture of smell and taste in Drosophila. *Annu Rev Neurosci* 30:505–533.

63. Kim H, Kirkhart C, Scott K (2017) Long-range projection neurons in the taste circuit of Drosophila. *eLife* 6. doi:10.7554/elife.23386.

64. Miyazaki T, Lin T-Y, Ito K, Lee C-H, Stopfer M (2015) A gustatory second-order neuron that connects sucrose-sensitive primary neurons and a distinct region of the gnathal ganglion in the Drosophila brain. *Journal of Neurogenetics* 29(2-3):144–155.

65. Kain P, Dahanukar A (2015) Secondary taste neurons that convey sweet taste and starvation in the Drosophila brain. *Neuron* 85(4):819–832.

66. Yarmolinsky DA, Zuker CS, Ryba NJP (2009) Common sense about taste: from mammals to insects. *Cell* 139(2):234–244.

67. Davis RL (2005) Olfactory memory formation in Drosophila: from molecular to systems neuroscience. *Annu Rev Neurosci* 28:275–302.

68. Keene AC, Waddell S (2007) Drosophila olfactory memory: single genes to complex neural circuits. *Nat Rev Neurosci* 8(5):341–354.

69. Schwaerzel M, et al. (2003) Dopamine and octopamine differentiate between aversive and appetitive olfactory memories in Drosophila. *J Neurosci* 23(33):10495–10502.

70. Burke CJ, et al. (2012) Layered reward signalling through octopamine and dopamine in Drosophila. *Nature* 492(7429):433–437.

71. Riemensperger T, Völler T, Stock P, Buchner E, Fiala A (2005) Punishment prediction by dopaminergic neurons in Drosophila. *Curr Biol* 15(21):1953–1960.

72. Mao Z, Davis RL (2009) Eight different types of dopaminergic neurons innervate the Drosophila mushroom body neuropil: anatomical and physiological heterogeneity. *Front Neural Circuits* 3:5.

73. Pool A-H, Scott K (2014) Feeding regulation in Drosophila. *Curr Opin Neurobiol* 29:57–63.

74. Kim Y-C, Lee H-G, Han K-A (2007) D1 dopamine receptor dDA1 is required in the mushroom body neurons for aversive and appetitive learning in Drosophila. *J Neurosci* 27(29):7640–7647.

75. Qin H, et al. (2012) Gamma neurons mediate dopaminergic input during aversive olfactory memory formation in Drosophila. *Curr Biol* 22(7):608–614.

76. Séjourné J, et al. (2011) Mushroom body efferent neurons responsible for aversive olfactory memory retrieval in Drosophila. *Nat Neurosci* 14(7):903–910.

77. Hattori D, et al. (2017) Representations of Novelty and Familiarity in a Mushroom Body Compartment. *Cell* 169(5):956–969.e17.

78. Lewis LPC, et al. (2015) A Higher Brain Circuit for Immediate Integration of Conflicting Sensory Information in Drosophila. *Curr Biol* 25(17):2203–2214.

79. Cohn R, Morantte I, Ruta V (2015) Coordinated and Compartmentalized Neuromodulation Shapes Sensory Processing in Drosophila. *Cell* 163(7):1742–1755.

80. Plaçais P-Y, Trannoy S, Friedrich AB, Tanimoto H, Preat T (2013) Two pairs of mushroom body efferent neurons are required for appetitive long-term memory retrieval in Drosophila. *Cell Rep* 5(3):769–780.

81. Pai T-P, et al. (2013) Drosophila ORB protein in two mushroom body output neurons is necessary for long-term memory formation. *Proc Natl Acad Sci U S A* 110(19):7898–7903.

82. Aso Y, Rubin GM (2016) Dopaminergic neurons write and update memories with cell-type-specific rules. *Elife* 5. doi:10.7554/eLife.16135.

83. Talay M, et al. (2017) Transsynaptic Mapping of Second-Order Taste Neurons in Flies by trans-Tango. *Neuron* 96(4):783–795.e4.

84. Hanesch U, -F. Fischbach K, Heisenberg M (1989) Neuronal architecture of the central complex in Drosophila melanogaster. *Cell and Tissue Research* 257(2):343–366.

85. Berry JA, Cervantes-Sandoval I, Chakraborty M, Davis RL (2015) Sleep Facilitates Memory by Blocking Dopamine Neuron-Mediated Forgetting. *Cell* 161(7):1656–1667.

86. Donlea JM, Thimgan MS, Suzuki Y, Gottschalk L, Shaw PJ (2011) Inducing sleep by remote control facilitates memory consolidation in Drosophila. *Science* 332(6037):1571–1576.

87. Ueno T, et al. (2012) Identification of a dopamine pathway that regulates sleep and arousal in Drosophila. *Nat Neurosci* 15(11):1516–1523.

88. Strauss R (2002) The central complex and the genetic dissection of locomotor behaviour. *Curr Opin Neurobiol* 12(6):633–638.

89. Liu G, et al. (2006) Distinct memory traces for two visual features in the Drosophila brain. *Nature* 439(7076):551–556.

90. Weir PT, Dickinson MH (2015) Functional divisions for visual processing in the central brain of flying Drosophila. *Proc Natl Acad Sci U S A* 112(40):E5523–32.

91. Sakai T, Kitamoto T (2006) Differential roles of two major brain structures, mushroom bodies and central complex, for Drosophila male courtship behavior. *J Neurobiol* 66(8):821–834.

92. Hu W, et al. (2018) Fan-Shaped Body Neurons in the Drosophila Brain Regulate Both Innate and Conditioned Nociceptive Avoidance. *Cell Rep* 24(6):1573–1584.

93. Gordon MD, Scott K (2009) Motor Control in a Drosophila Taste Circuit. *Neuron* 61(3):373–384.

94. Manzo A, Silies M, Gohl DM, Scott K (2012) Motor neurons controlling fluid ingestion in Drosophila. *Proc Natl Acad Sci U S A* 109(16):6307–6312.

95. Mann K, Gordon MD, Scott K (2013) A Pair of Interneurons Influences the Choice between Feeding and Locomotion in Drosophila. *Neuron* 79(4):754–765.

96. Marella S, Mann K, Scott K (2012) Dopaminergic Modulation of Sucrose Acceptance Behavior in Drosophila. *Neuron* 73(5):941–950.

97. Yamagata N, et al. (2015) Distinct dopamine neurons mediate reward signals for short- and long-term memories. *Proceedings of the National Academy of Sciences* 112(2):578–583.

98. Huetteroth W, et al. (2015) Sweet taste and nutrient value subdivide rewarding dopaminergic neurons in Drosophila. *Curr Biol* 25(6):751–758.

99. Ichinose T, et al. (2015) Reward signal in a recurrent circuit drives appetitive long-term memory formation. *eLife* 4. doi:10.7554/elife.10719.

100. Klapoetke NC, et al. (2014) Addendum: independent optical excitation of distinct neural populations. *Nat Methods* 11(9):972.

101. Kitamoto T (2001) Conditional modification of behavior in Drosophila by targeted expression of a temperature-sensitive shibire allele in defined neurons. *J Neurobiol* 47(2):81–92.

102. Pfeiffer BD, Truman JW, Rubin GM (2012) Using translational enhancers to increase transgene expression in Drosophila. *Proc Natl Acad Sci U S A* 109(17):6626–6631.

103. Mohamed GA, et al. (2017) Optical inhibition of larval zebrafish behaviour with anion channelrhodopsins. *BMC Biol* 15(1):103.

104. Baines RA, Uhler JP, Thompson A, Sweeney ST, Bate M (2001) Altered electrical properties in Drosophila neurons developing without synaptic transmission. *J Neurosci* 21(5):1523–1531.

105. Pfeiffer BD, et al. (2010) Refinement of tools for targeted gene expression in Drosophila. *Genetics* 186(2):735–755.

106. Wu M, et al. (2016) Visual projection neurons in the Drosophila lobula link feature detection to distinct behavioral programs. *eLife* 5. doi:10.7554/elife.21022.

107. Shang Y, Griffith LC, Rosbash M (2008) Light-arousal and circadian photoreception circuits intersect at the large PDF cells of the Drosophila brain. *Proc Natl Acad Sci U S A* 105(50):19587–19594.

108. Simpson JH (2016) Rationally subdividing the fly nervous system with versatile expression reagents. *J Neurogenet* 30(3-4):185–194.

109. Dana H, et al. (2019) High-performance calcium sensors for imaging activity in neuronal populations and microcompartments. *Nature Methods* 16(7):649–657.

110. Branson K, Robie AA, Bender J, Perona P, Dickinson MH (2009) High-throughput ethomics in large groups of Drosophila. *Nat Methods* 6(6):451–457.

111. Harris DT, Kallman BR, Mullaney BC, Scott K (2015) Representations of Taste Modality in the Drosophila Brain. *Neuron* 86(6):1449–1460.

112. Cajal SR y. (1909) Histologie du système nerveux de l'homme & des vertébrés. doi:10.5962/bhl.title.48637.

113. Hebb DO (1949) The organization of behavior: A neuropsychological theory.

114. Bliss TV, Lomo T (1973) Long-lasting potentiation of synaptic transmission in the dentate area of the anaesthetized rabbit following stimulation of the perforant path. *J Physiol* 232(2):331–356.

115. Bliss TV, Gardner-Medwin AR (1973) Long-lasting potentiation of synaptic transmission in the dentate area of the unanaestetized rabbit following stimulation of the perforant path. *J Physiol* 232(2):357–374.

116. Nicoll RA (2017) A Brief History of Long-Term Potentiation. *Neuron* 93(2):281–290.

117. Maffei A (2018) Long-Term Potentiation and Long-Term Depression. *Oxford Research*

Encyclopedia of Neuroscience. doi:10.1093/acrefore/9780190264086.013.148.

118. Trimmer JS, Rhodes KJ (2004) Localization of voltage-gated ion channels in mammalian brain. *Annu Rev Physiol* 66:477–519.

119. Helmchen F, Imoto K, Sakmann B (1996) Ca2+ buffering and action potential-evoked Ca2+ signaling in dendrites of pyramidal neurons. *Biophys J* 70(2):1069–1081.

120. Grienberger C, Konnerth A (2012) Imaging Calcium in Neurons. *Neuron* 73(5):862–885.

121. Hamel EJO, Grewe BF, Parker JG, Schnitzer MJ (2015) Cellular Level Brain Imaging in Behaving Mammals: An Engineering Approach. *Neuron* 86(1):140–159.

122. Liman ER, Zhang YV, Montell C (2014) Peripheral coding of taste. *Neuron* 81(5):984–1000.

123. Kim H, Kirkhart C, Scott K (2017) Long-range projection neurons in the taste circuit of. *Elife* 6. doi:10.7554/eLife.23386.

124. Marella S, et al. (2006) Imaging taste responses in the fly brain reveals a functional map of taste category and behavior. *Neuron* 49(2):285–295.

125. Musso P-Y, et al. (2019) Closed-loop optogenetic activation of peripheral or central neurons modulates feeding in freely moving. *Elife* 8. doi:10.7554/eLife.45636.